Journal of Virology

Enhanced Potency of a Broadly Neutralizing HIV-1 Antibody *In Vitro* Improves Protection against Lentiviral Infection *In Vivo*

Rebecca S. Rudicell, Young Do Kwon, Sung-Youl Ko, Amarendra Pegu, Mark K. Louder, Ivelin S. Georgiev, Xueling Wu, Jiang Zhu, Jeffrey C. Boyington, Xuejun Chen, Wei Shi, Zhi-yong Yang, Nicole A. Doria-Rose, Krisha McKee, Sijy O'Dell, Stephen D. Schmidt, Gwo-Yu Chuang, Aliaksandr Druz, Cinque Soto, Yongping Yang, Baoshan Zhang, Tongqing Zhou, John-Paul Todd, Krissey E. Lloyd, Joshua Eudailey, Kyle E. Roberts, Bruce R. Donald, Robert T. Bailer, Julie Ledgerwood, NISC Comparative Sequencing Program, James C. Mullikin, Lawrence Shapiro, Richard A. Koup, Barney S. Graham, Martha C. Nason, Mark Connors, Barton F. Haynes, Srinivas S. Rao, Mario Roederer, Peter D. Kwong, John R. Mascola and Gary J. Nabel

J. Virol. **2014, 88(21):12669. DOI: 10.1128/JVI.02213-14.**
Published Ahead of Print 20 August 2014.

JVI Journals.ASM.org

Enhanced Potency of a Broadly Neutralizing HIV-1 Antibody *In Vitro* Improves Protection against Lentiviral Infection *In Vivo*

Rebecca S. Rudicell,[a]* Young Do Kwon,[a] Sung-Youl Ko,[a] Amarendra Pegu,[a] Mark K. Louder,[a] Ivelin S. Georgiev,[a] Xueling Wu,[a]* Jiang Zhu,[a]* Jeffrey C. Boyington,[a] Xuejun Chen,[a] Wei Shi,[a] Zhi-yong Yang,[a]* Nicole A. Doria-Rose,[a] Krisha McKee,[a] Sijy O'Dell,[a] Stephen D. Schmidt,[a] Gwo-Yu Chuang,[a] Aliaksandr Druz,[a] Cinque Soto,[a] Yongping Yang,[a] Baoshan Zhang,[a] Tongqing Zhou,[a] John-Paul Todd,[a] Krissey E. Lloyd,[b] Joshua Eudailey,[b] Kyle E. Roberts,[c] Bruce R. Donald,[c,d] Robert T. Bailer,[a] Julie Ledgerwood,[a] NISC Comparative Sequencing Program,[e] James C. Mullikin,[e] Lawrence Shapiro,[a,f] Richard A. Koup,[a] Barney S. Graham,[a] Martha C. Nason,[g] Mark Connors,[h] Barton F. Haynes,[b] Srinivas S. Rao,[a] Mario Roederer,[a] Peter D. Kwong,[a] John R. Mascola,[a] Gary J. Nabel[a]*

Vaccine Research Center, National Institute of Allergy and Infectious Diseases, National Institutes of Health, Bethesda, Maryland, USA[a]; Duke Human Vaccine Institute, Duke University Medical Center, Durham, North Carolina, USA[b]; Department of Computer Science, Duke University, Durham, North Carolina, USA[c]; Department of Biochemistry, Duke University Medical Center, Durham, North Carolina, USA[d]; NIH Intramural Sequencing Center, National Human Genome Research Institute, National Institutes of Health, Bethesda, Maryland, USA[e]; Department of Biochemistry and Molecular Biophysics, Columbia University, New York, New York, USA[f]; Biostatistics Research Branch, National Institute of Allergy and Infectious Diseases, National Institutes of Health, Bethesda, Maryland, USA[g]; HIV-Specific Immunity Section, Laboratory of Immunoregulation, National Institute of Allergy and Infectious Diseases, National Institutes of Health, Bethesda, Maryland, USA[h]

ABSTRACT

Over the past 5 years, a new generation of highly potent and broadly neutralizing HIV-1 antibodies has been identified. These antibodies can protect against lentiviral infection in nonhuman primates (NHPs), suggesting that passive antibody transfer would prevent HIV-1 transmission in humans. To increase the protective efficacy of such monoclonal antibodies, we employed next-generation sequencing, computational bioinformatics, and structure-guided design to enhance the neutralization potency and breadth of VRC01, an antibody that targets the CD4 binding site of the HIV-1 envelope. One variant, VRC07-523, was 5- to 8-fold more potent than VRC01, neutralized 96% of viruses tested, and displayed minimal autoreactivity. To compare its protective efficacy to that of VRC01 *in vivo*, we performed a series of simian-human immunodeficiency virus (SHIV) challenge experiments in nonhuman primates and calculated the doses of VRC07-523 and VRC01 that provide 50% protection (EC_{50}). VRC07-523 prevented infection in NHPs at a 5-fold lower concentration than VRC01. These results suggest that increased neutralization potency *in vitro* correlates with improved protection against infection *in vivo*, documenting the improved functional efficacy of VRC07-523 and its potential clinical relevance for protecting against HIV-1 infection in humans.

IMPORTANCE

In the absence of an effective HIV-1 vaccine, alternative strategies are needed to block HIV-1 transmission. Direct administration of HIV-1-neutralizing antibodies may be able to prevent HIV-1 infections in humans. This approach could be especially useful in individuals at high risk for contracting HIV-1 and could be used together with antiretroviral drugs to prevent infection. To optimize the chance of success, such antibodies can be modified to improve their potency, breadth, and *in vivo* half-life. Here, knowledge of the structure of a potent neutralizing antibody, VRC01, that targets the CD4-binding site of the HIV-1 envelope protein was used to engineer a next-generation antibody with 5- to 8-fold increased potency *in vitro*. When administered to nonhuman primates, this antibody conferred protection at a 5-fold lower concentration than the original antibody. Our studies demonstrate an important correlation between *in vitro* assays used to evaluate the therapeutic potential of antibodies and their *in vivo* effectiveness.

Pathogen-specific antibodies can prevent infection by numerous human viruses (1, 2). For HIV-1, neutralizing antibodies to the gp120 and gp41 envelope glycoproteins (Env) can prevent infection in the macaque simian/human immunodeficiency virus (SHIV) model of infection (3–10). Initial studies suggested high levels of antibodies were required for protection, but more recent studies suggest that lower, physiologically achievable levels of plasma antibody can prevent infection by mucosal challenge (8, 9, 11). While no human passive prevention studies have been conducted with HIV-1-specific neutralizing monoclonal antibodies (MAbs) so far, the available animal model data suggest that neutralizing antibodies induced by a vaccine or passive immunization could prevent human HIV-1 infection (12, 13). Advances in B-cell immunology and cloning techniques have led to the isolation of numerous HIV-1 neutralizing MAbs with potency and breadth far greater than those of earlier antibodies. These antibodies target multiple sites of vulnerability on HIV-1 Env (14), including the

Received 29 July 2014 **Accepted** 14 August 2014

Published ahead of print 20 August 2014

Editor: R. W. Doms

Address correspondence to John R. Mascola, jmascola@nih.gov, or Gary J. Nabel, gary.nabel@sanofi.com.

* Present address: Rebecca S. Rudicell, Sanofi, Cambridge, Massachusetts, USA; Xueling Wu, Aaron Diamond AIDS Research Center, The Rockefeller University, New York, New York, USA; Jiang Zhu, The Scripps Research Institute, La Jolla, California, USA; Zhi-yong Yang, Sanofi, Cambridge, Massachusetts, USA; Gary J. Nabel, Sanofi, Cambridge, Massachusetts, USA.

R.S.R. and Y.D.K. contributed equally.

Supplemental material for this article may be found at http://dx.doi.org/10.1128/JVI.02213-14.

doi:10.1128/JVI.02213-14

CD4 binding site (CD4bs), the V1V2 region, a glycan V3 site of gp120, the membrane-proximal external region of gp41, and three newly described sites that include regions of both gp120 and gp41 (15–38).

Among these MAbs is VRC01, a CD4-binding site-directed antibody that neutralizes ~90% of HIV-1 strains with a 50% inhibitory concentration (IC_{50}) of less than 50 μg/ml and 72% of HIV-1 strains with an IC_{50} of less than 1 μg/ml (19). The crystal structure of VRC01 bound to gp120 reveals a mode of antibody recognition similar to the recognition of gp120 by the cell surface receptor CD4 (20). Additional MAbs that share genetic and structural characteristics with VRC01 have been discovered (24, 26, 39), and these MAbs have been collectively termed the VRC01 class of neutralizing antibodies (14, 34, 40). VRC01 is able to protect macaques against vaginal or rectal SHIV challenge (41), a topical gel formulation is able to protect humanized mice from HIV-1 challenge (42), and gene-based production of VRC01 from an adeno-associated virus vector is able to protect humanized mice against HIV-1 infection (43, 44). Together, these data suggest that VRC01 may prevent infection in humans.

In addition to their potential to prevent infection, HIV-1 MAbs may have a role as therapeutic agents. Several recent studies in NHP (45, 46) and humanized mouse models (47, 48) indicate that combinations of potent HIV-1 MAbs substantially reduce plasma viremia. These studies also suggested that the magnitude of the *in vivo* therapeutic effect on viremia was related to the *in vitro* neutralization potency of the antibodies. Prior NHP studies also have suggested that infection could be prevented by passive infusion of neutralizing, but not nonneutralizing, HIV-1-specific antibodies (3, 49, 50).

We hypothesized that the *in vitro* neutralization potency of an HIV-1-specific MAb would correlate with its ability to prevent infection *in vivo*; therefore, we sought to improve the neutralization potency and breadth of reactivity of antibody VRC01. Although various HIV-1 specific MAbs, including new, more potent MAbs (11, 41), have been evaluated in NHPs, a direct comparison between a wild-type and a higher potency engineered variant has not been performed. Here, we used next-generation sequencing of antibody gene transcripts to identify heavy-chain somatic variants of VRC01 with enhanced neutralization potency. The somatic variant with highest potency, VRC07, was subjected to an iterative process of computational and structure-guided optimization which identified mutations that optimized neutralization potency and minimized autoreactivity *in vitro*. This process led to the selection of next-generation VRC07 variants that allowed us to determine whether increased virus neutralization *in vitro* conferred greater protection against infectious challenge *in vivo*. The definition of the correlates and mechanisms of antibody-mediated protection has significant implications for the development of effective immunoprophylaxis against HIV-1 infection.

MATERIALS AND METHODS

Human specimens. The peripheral blood mononuclear cells (PBMCs) used in this study were obtained from the HIV-1-infected donor 45 who enrolled in Institutional Review Board-approved clinical protocols at the National Institute of Allergy and Infectious Diseases (NIAID). The anti-HIV-1 broadly neutralizing MAbs VRC01, VRC02, VRC03, NIH45-46, NIH45-177, NIH45-243, VRC06, and VRC06b (19, 24, 51) were isolated from this donor from PBMCs collected in 2008, which was 18 years after his diagnosis of HIV-1 clade B infection in 1990. Donor 45 was a slow progressor and remained antiretroviral treatment naïve, with CD4 T-cell counts of over 500 cells/μl and plasma HIV-1 RNA loads of less than 15,000 copies/ml.

Sample preparation for 454 pyrosequencing. The 454 library preparation and pyrosequencing of heavy-chain transcripts was performed at the NIH Sequencing Center (NISC) as previously described (26). Briefly, mRNA was extracted from 20 million PBMCs into 200 μl elution buffer using the Oligotex direct mRNA minikit (Qiagen) and then concentrated to 10 to 30 μl by centrifuging the buffer through a Microcon 30-kDa filter (Millipore). Reverse transcription was performed in one or multiple 35-μl reaction mixtures, each composed of 13 μl of mRNA, 3 μl of oligo$(dT)_{12-18}$ at 0.5 μg/μl (Invitrogen), 7 μl of 5× first-strand buffer (Invitrogen), 3 μl of RNaseOut (Invitrogen), 3 μl of 0.1 M dithiothreitol (DTT; Invitrogen), 3 μl of deoxynucleoside triphosphate (dNTP) mix (each at 10 mM), and 3 μl of SuperScript II (Invitrogen). The reaction mixtures were incubated at 42°C for 2 h. The cDNAs from each reaction were combined, applied to the NucleoSpin extract II kit (Clontech), and eluted in 20 μl of elution buffer. In this way, 1 μl of the cDNA comprised transcripts from one million PBMCs. The immunoglobulin VH1 gene family PCR was set up in a total volume of 50 μl, using 5 μl of the cDNA as the template (equivalent of transcripts from 5 million PBMCs). The DNA polymerase system used was the Platinum *Taq* high-fidelity (HiFi) system (Invitrogen). In accordance with the manufacturer's instructions, the reaction mix was composed of water, 5 μl of 10× buffer, 1 μl of supplied $MgSO_4$, 2 μl of dNTP mix (each at 10 mM), 1 to 2 μl of primers at 25 μM, and 1 μl of Platinum *Taq* HiFi DNA polymerase. The forward primers for VH1 gene amplification were a mix of the following: 5′L-VH1, 5′-ACAGGTGCCCACTCCCAGGTGCAG-3′; 5′L-VH1#2, 5′-GCAGCCACAGGTGCCCACTCC-3′; 5′L-VH1-24, 5′-CAGCAGCTACAGGCACCCACGC-3′; and 5′L-VH1-69, 5′-GGCAGCAGCTACAGGTGTCCAGTCC-3′. The reverse primers were 3′Cγ-CH1 (5′-GGGGGAAGACCGATGGGCCCTTGGTGG-3′) and 3′Cμ-CH1 (5′-GGGAATTCTCACAGGAGACGA-3′). We should note that the VH1 forward primers used for this PCR were based on the unmutated germ line human VH1 gene sequences, annealing at the 3′ end of the leader region or at the first three residues in the coding region. For heavily somatically hypermutated heavy-chain sequences, such as those found in the VRC01 class, somatic hypermutations in these regions will affect the PCR amplification efficiency as reported previously (24). The PCRs were initiated at 95°C for 30 s, followed by 25 cycles of 95°C for 30 s, 58°C for 30 s, and 72°C for 1 min, and then a final incubation at 72°C for 10 min. The PCR products at the expected size (~500 bp) were gel extracted and purified (Qiagen), followed by further phenol-chloroform extraction (52).

454 Library preparation and pyrosequencing. Sample preparation and 454 pyrosequencing of heavy- and light-chain transcripts was performed as previously described (26). The PCR product was quantified using Qubit (Life Technologies, Carlsbad, CA). Following end repair, 454 adapters were added by ligation. Library concentrations were determined using the KAPA Biosystems quantitative PCR (qPCR) system (Woburn, MA) with 454 pyrosequencing standards provided in the KAPA system. Pyrosequencing of the PCR products was performed on a GS FLX sequencing instrument (Roche 454 Life Sciences, Bradford, CT) using the manufacturer's suggested methods and reagents. Initial image collection was performed on the GS FLX instrument, and subsequent signal processing, quality filtering, and generation of nucleotide sequence and quality scores were performed on an off-instrument Linux cluster using 454 application software (version 2.5.3).

Bioinformatics analysis of 454 pyrosequencing reads. A general bioinformatics pipeline was developed in-house to process and analyze 454 pyrosequencing reads. Specifically, each sequence read was (i) reformatted and labeled with a unique index number; (ii) assigned to the variable (V) gene family and allele using an in-house implementation of IgBLAST (http://www.ncbi.nlm.nih.gov/igblast/) (sequences with an E value or $>10^{-3}$ were rejected); (iii) compared to the germ line V gene and known VRC01-like antibodies using nucleotide sequences and a global alignment module implemented in CLUSTALW2 (53), which provides

the basis for identity/divergence-grid analysis; and (iv) subjected to a template-based error correction scheme where 454 homopolymer errors in the V gene were detected and corrected based on the alignment to the germ line sequence. The VRC07 heavy-chain sequence was identified based on its 90% nucleotide sequence identity to the VRC01 heavy chain.

Numbering of amino acid residues in antibody. We followed the Kabat (54) or the IMGT (http://www.imgt.org/) nomenclature for amino acid sequences in antibodies as indicated.

Generation of VRC07 and mutants. Plasmids encoding the heavy and light chains of VRC07 and related variants were generated either by gene synthesis (Genscript, Piscataway, NJ, or GeneImmune, Rockville, MD) or site-directed mutagenesis (QuikChange II XL site-directed mutagenesis kit or QuikChange lightning multisite-directed mutagenesis kit; Agilent). All MAbs were expressed by transiently cotransfecting the heavy and light chains into HEK 293F cells. Supernatants were harvested 5 to 6 days later, and IgG was purified with protein A or protein G affinity chromatography (GE Healthcare).

Crystallization, data collection, and structure determination. The VRC07 heavy-chain gene with an HRV3C cleavage site (GLEVLFQGP) after Lys 235 was synthesized and cloned into the pVRC8400 vector. The VRC01 light-chain gene was synthesized and cloned into the same vector, and an Asn72Thr mutation was introduced to remove a glycosylation site. Antigen binding fragments (Fabs) were prepared by digestion of IgGs with HRV3C protease as described previously (22). Clade A/E 93TH057 gp120 extended core ($core_e$) was prepared as reported previously (55). Fab-93TH057gp120 $core_e$ complexes were further purified using Superdex 200 16/60 (GE Healthcare) and concentrated to ~10 mg/ml in buffer containing 2.5 mM, Tris-HCl, pH 7.5, 350 mM NaCl, 0.02% NaN_3. Initial crystallizations were performed using a Honeybee 963 robot and a commercially available Hampton screen (Hampton Research), Precipitant Synergy screen (Emerald Biosystems), and Wizard screen (Emerald Biosystems). Crystallization conditions were further optimized manually. Crystals suitable for diffraction grew in a vapor diffusion hanging-drop setup by mixing 0.5 μl of protein and 0.5 μl of reservoir solutions containing 10 to 14% polyethylene glycol (PEG) 4000, 0.2 M sodium acetate, 0.1 M Tris-HCl, pH 8.5. X-ray diffraction data were collected at the synchrotron beamlines (Advanced Photon Source, Argonne National Laboratory) SER-CAT ID22 and BM22 from crystals in cryoprotectant containing 15% ethylene glycol, 15% glycerol, and 7.5% 2R,3R-butanediol and then supplemented with reservoir solutions. Data were processed using HKL2000 (56). The structures were determined by molecular replacement using Phaser (57) and VRC01-bound 93TH057gp120 (PDB entry 3NGB) as the search model. Models were rebuilt manually using COOT (58), and refinement was performed with PHENIX (59). The program PISA (60) was used to calculate binding surfaces.

Structure-guided optimizations. (i) Design of VRC07 heavy-chain interface mutants. All VRC07-gp120 interface residues of the Ab were considered for mutation. For each amino acid position, a structure-based design was conducted using OSPREY (61, 62). The top-ranked OSPREY mutants were visualized for gained interface interactions using Probe (63) and selected for mutagenesis.

(ii) Design of VRC07 partial framework reversions to germ line. A method for partial reversion of antibody residues to the germ line was used as described previously (64). Specific amino acids in the variable heavy- and variable light-framework regions were chosen for reversion to germ line. Structural analysis and structure-based design were performed using OSPREY (61, 62), MolProbity (65), and PyMOL (PyMOL Molecular Graphics System, version 1.5.0.4; Schrödinger, LLC).

(iii) Design of VRC07 mutants with altered hydrophobic residues. Hydrophobic residues that were exposed on the VRC07 surface but that were not part of the antibody-gp120 interface were selected for mutation. The solvent-accessible surface area for each residue was computed using ASA-View (66), and antibody-antigen analysis was performed using PISA (60). Additional mutations to Asp or Glu in the heavy-chain second complementarity determining region (CDR H2) and CDR L1 were introduced to improve biophysical properties (67). Structure-based antibody redesign and mutation scoring was performed using OSPREY (61, 62).

(iv) Redesign of VRC07 light-chain–heavy-chain interface. The following VRC07 light-chain residues at the interface with the antibody heavy chain, but not proximal to gp120, were selected for redesign: Ala34, Ala43, Leu46, Ala55, and Ala56. The OSPREY protein redesign software (61, 62) was used to search for and select mutations at these residue positions that may stabilize the VRC07 light-chain–heavy-chain interface.

(v) Design of G54 mutants. Initially, G54 variants were selected based on information gained from previous reports (19, 26, 68) and current structural studies. The rationale was to select residues with bulky hydrophobic side chains, such as Phe, Trp, or Tyr, that will allow mimicry of the gp120-Phe 43_{CD4} interaction. The initial G54F, G54W, and G54Y variants showed increased potency and breadth but also showed strong autoreactivity. Thus, we generated variants with all possible amino acids at this location and tested their neutralization potency/breadth and autoreactivity.

(vi) Design of light-chain N-terminal modifications. A close inspection of the previous (20) and current VRC07-bound gp120 structures revealed that the most N-terminal region of the VRC01 light chain was disordered and did not contact gp120. Furthermore, it was likely that the N terminus of the light chain would encounter a clash with HIV-1 strains possessing a long V5 region. To negate the potential structural clashes, we designed the light-chain variants with various N-terminal residues truncated and/or replaced with Gly or Ala. At later stages, we also generated the light-chain variants with Ser or Glu replaced at position 3 to reduce autoreactivity.

(vii) Analyses of variants. All variants were expressed as IgG1 and tested for neutralization breadth/potency and/or autoreactivity. Results were used to generate new rounds of mutations. Promising modifications were down-selected and combined.

Neutralization analysis. Neutralization was measured using single-round-of-infection HIV-1 Env pseudoviruses and TZM-bl target cells (HeLa cells engineered to express CD4 and CCR5), as described previously (19, 70–72). Neutralization curves were fit by nonlinear regression using a 5-parameter Hill slope equation. The 50% and 80% inhibitory concentrations (IC_{50} and IC_{80}) were reported as the antibody concentration or serum dilution required to inhibit infection by 50% and 80%, respectively.

VRC07 G54 variant ELISA. The binding of VRC07 G54 variants to HIV-1 gp120 protein (consensus sequence protein for clade A1; Immune Technology Corp., New York, NY) was detected with enzyme-linked immunosorbent assay (ELISA). Briefly, Nunc MaxiSorp plates (Thermo Fisher) were coated overnight with 2 μg/ml of HIV-1 gp120 protein (Con_A1; Immune Technology Corp., New York, NY) in phosphate-buffered saline (PBS) (pH 7.4). Coated plates were blocked with PBS-Tween 20 (PBS-T) buffer containing 5% skim milk (Thermo Fisher) and 2% bovine albumin fraction V (MP Biomedicals, Santa Ana, CA) for 1 h at room temperature (RT) or overnight at 4°C, followed by incubation with antibody serially diluted in PBS-T buffer for 1 h at RT. Horseradish peroxidase-conjugated sheep anti-human IgG antibody (GE Healthcare) at 1:5,000 was added for 1 h at RT. All volumes were 100 μl/well, except that 200 μl/well was used for blocking. Plates were washed five times between each step with PBS-T. After a final wash, plates were developed using 100 μl/well of 3,3′,5,5′-tetramethylbenzidine (TMB) (Kirkegaard & Perry Laboratories, Gaithersburg, MD), stopped using 50 μl/well of 0.5 M NaOH, and read at 450 nm.

Polyreactivity analysis of antibodies. Antibody binding to cardiolipin was determined as previously described (73). Briefly, using the QUANTA Lite ACA IgG III ELISA kit (Zeus Scientific) per the manufacturer's protocol, each antibody was diluted to 100 μg/ml in the kit sample diluent and tested in 3-fold serial dilutions. Results shown are representative of at least two independent ELISAs. Positive and negative controls were included on each plate, and values three times above the background were considered positive. Antibody reactivity to a human epithelial cell

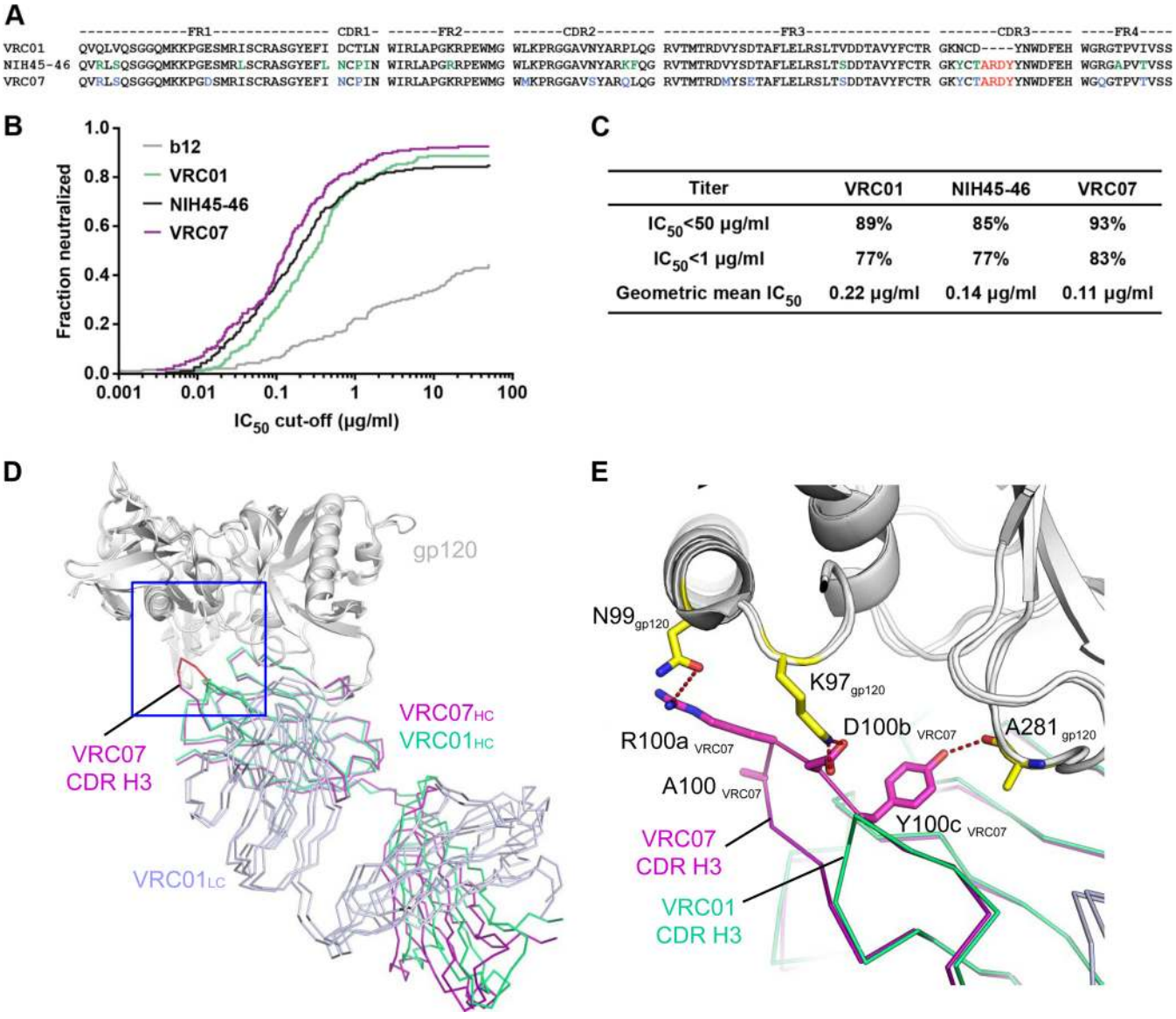

FIG 1 VRC07 is a more potent clonal relative of VRC01. (A) An alignment of VRC01, NIH45-46, and VRC07 heavy-chain variable regions highlights the four-amino-acid insertion in the CDR H3 (red). Additional amino acid changes from VRC01 are highlighted in green (NIH45-46) and blue (VRC07). (B) VRC07 neutralization was assessed on a panel of 179 viral strains. For comparison, b12, VRC01, and NIH45-46 also were analyzed. Potency-breadth curves show the fraction of viruses neutralized at increasing IC_{50} cutoff values. (C) The percentage of viruses neutralized with an IC_{50} of less than 50 μg/ml and less than 1 μg/ml are listed for VRC01, NIH45-46, and VRC07. (D) Superposition of the VRC01 and VRC07 antibody-bound gp120 structures. The VRC07 heavy chain is in purple, the VRC01 heavy chain is shown in green, and both light chains are shown in light purple. VRC01 and VRC07 adopt the same modes of gp120 recognition, while the four-amino-acid insertion (highlighted in red) in the CDR H3 of VRC07 makes additional contacts with gp120 (gray). (E) Closeup view of interactions (marked as a square box in panel D) between gp120 and the CDR H3 loop of VRC07. Hydrogen bonds and electrostatic interactions (dashed line in red) were found between gp120 and R100a, D100b, and Y100c of VRC07.

line (HEp-2) was determined with the ANA/HEp-2 cell culture immunofluorescence assay (IFA) test system (Zeus Scientific) per the manufacturer's protocol and as previously described (73). Antibodies were diluted to 50 μg/ml and 25 μg/ml in ZOBRA-NS diluent. Positive and negative controls were included on each slide. Antibodies were scored negative or positive (1+ to 4+) at each dilution. Results are representative of at least two independent experiments.

Animals. Male *Macaca mulatta* animals of Indian origin were used in these studies. All animal experiments were reviewed and approved by the Animal Care and Use Committee of the Vaccine Research Center, NIAID, NIH, and all animals were housed and cared for in accordance with local, state, federal, and institute policies in an American Association for Accreditation of Laboratory Animal Care-accredited facility at the NIH.

Pharmacokinetics in nonhuman primates. Indian rhesus macaques were infused intravenously with 10 mg of MAb/kg of body weight. Endotoxin levels were measured for each antibody preparation by the QCL-1000 endpoint chromogenic *Limulus* amebocyte lysate (LAL) assay (Lonza), and all were below 0.5 EU/mg. Whole-blood samples were collected prior to injection and at time points 0, 30 min, 6 h, 12 h, and days 1, 2, 4, 7, 14, 21, and 28. Plasma was separated by centrifugation. Plasma samples were heat inactivated at 56°C for 30 min, and lipoproteins were

pelleted. Plasma MAb levels were determined by RSC3 (resurfaced stabilized gp120 core, derivative 3) ELISA (described below).

ELISA to determine plasma antibody concentration. Plasma MAb levels were quantified using plates coated with RSC3 (19). Briefly, Nunc MaxiSorp (Thermo Fisher) plates were coated overnight with 200 ng/well of RSC3 in PBS, washed with PBS-T five times, and blocked with a blocking buffer of Tris-buffered saline-Tween 20 (TBS-T) with 5% milk and 2% bovine serum albumin (BSA) for at least 1 h. Five-fold serial dilutions ranging from 1:5 to 1:62,500 of plasma were made in blocking buffer. For each sample, three consecutive serial dilutions were plated in duplicate. An antibody-specific standard curve (starting at 200 ng/ml with eight 2.5-fold serial dilutions) and positive, negative, and spiked controls were included on each plate. Plasma was incubated on the plate for 1 h at RT, followed by a PBS-T wash. Bound MAbs were probed with a horseradish peroxidase-labeled goat anti-human IgG (1:5,000 dilution; Jackson Laboratories) for 30 min at RT. The plate was washed, and 100 μl SureBlue TMB (Kirkegaard & Perry Laboratories, Gaithersburg, MD) substrate was added. Once color was developed (typically 15 to 20 min), stopping buffer (100 μl 1N H_2SO_4) was added and the optical density at 450 nm was read. Softmax Pro V5.2revC (Molecular Devices) software was used to calculate MAb concentrations.

Pharmacokinetic calculations. Pharmacokinetic parameters were calculated by WinNonlin software (Pharsight) using a noncompartmental model.

Mucosal sampling. Rectal mucosal samples were collected by Weck-Cel sponges (Beaver Visitec) (5). Three samples were collected per animal per time point, and sponges were stored at −80°C until processing. All samples with visible blood were discarded. To elute mucosal samples, sponges were placed in Spin-X columns (Corning) on ice, 300 μl chilled elution buffer (PBS with protease inhibitor, 10% IGEPAL, and 0.25% BSA) was added, and samples were spun at 13,000 × *g* for 15 min at 4°C. MAb levels in eluted mucosal samples were quantified by RSC3 ELISA.

Passive transfer experiments. Endotoxin-free VRC01-LS (0.3 mg/kg, $n = 12$), VRC07-523-LS (0.2 mg/kg, $n = 4$, and 0.05 mg/kg, $n = 4$), or control IgG (purified, pooled human IgG; Sigma) (0.2 mg/kg, $n = 4$) was administered intravenously into male rhesus macaques that were intrarectally challenged 5 days later with 1 ml of undiluted SHIV BaLP4 stock virus (50% infective dose [$TCID_{50}$] titer of 12,800/ml in the TZM-bl assay) (41, 74), which routinely infects animals after a single dose. Plasma from blood collected just prior to challenge was used to determine the concentration of MAb at the time of challenge. After challenge, weekly blood samples were collected to determine infection status by viral load analysis. Of note, all four control animals became infected.

Plasma viral RNA. Plasma viral RNA (copies/ml) was determined by the Duke Human Vaccine Institute Immunology and Virology Quality Assessment Center using a Qiagen QIAsymphony Virus/Pathogen Midi Kit and a QIAgility Applied Biosystems StepOne quantitative real-time PCR.

Calculations of the probability of protection. The probability of protection is modeled as a function of the logarithm of MAb concentration at the day of challenge using generalized linear models with probit link functions (75). Separate models were fit for VRC01-LS and VRC07-523-LS, with an additional model combining data from both antibodies to test for a difference between the two. Ninety percent pointwise confidence curves for each model are built from empirical quantiles based on refitting the individual models to 10,000 bootstrapped samples.

Accession numbers. The coordinates and structure factors for the gp120-VRC07 antibody complex structures reported in this paper have been deposited with the Protein Data Bank (PDB codes 4OLU, 4OLV, 4OLW, 4OLX, 4OLY, 4OLZ, 4OM0, and 4OM1). We have also deposited deep-sequencing data for donor 45 used in this study to the NCBI Sequence Read Archive (SRA) under accession no. SRP04860. Relevant variable region sequences for VRC07, VRC07-501, VRC07-508, VRC07-523, and VRC07-544 were deposited with GenBank (accession numbers KM408142 and KM408147 to KM408150), as were sequences 45-08-110497H, 45-08-212510H, 45-08-511533H, and 45-08-541880H in Fig. S1 (accession numbers KM408143 to KM408146).

RESULTS

VRC07 is a clonal relative of VRC01 with increased neutralization potency. Our prior studies indicated that VRC01, isolated from donor 45, was a member of a clonal family of antibodies that included VRC02 and VRC03 (26, 34). To identify more potent variants of this clonal lineage, we performed 454 pyrosequencing of antibody-gene transcripts (26, 76) from peripheral blood B cells of donor 45, the source of VRC01-03 (19, 26). VH1 gene family-specific primers yielded mostly heavy-chain transcripts related to VRC03, but four sequences were similar to VRC01 (26) (see Fig. S1 in the supplemental material). Two of these were identical, revealing a heavy-chain sequence that shared 90% nucleotide sequence identity to VRC01 but differing at 15 amino acid positions and containing a four-amino-acid insertion in the heavy-chain third complementarity determining region (CDR H3) (Fig. 1A). While the natural light-chain partner of this sequence was not obtained from heavy-chain PCR amplification and pyrosequencing, our previous studies demonstrated efficient light-chain complementation among VRC01 class antibodies (26). Thus, this heavy chain was paired with the original VRC01 light chain for protein expression as a full IgG1. The resulting MAb was named VRC07.

The neutralization activity of VRC07 was assessed on a panel of 179 diverse HIV-1 Env pseudoviruses that included 20 VRC01-resistant strains. MAb NIH45-46, another clonal variant of VRC01, was included for comparison because it also contains a four-amino-acid CDR H3 insert (24) similar to that of VRC07 (Fig. 1A). VRC07 neutralized a greater fraction of viruses than VRC01 or NIH45-46 at all tested concentrations (Fig. 1B). Overall, VRC07 neutralized 93% of strains with an IC_{50} of less than 50 μg/ml and 83% of strains with an IC_{50} of less than 1 μg/ml and was able to neutralize 8 of 20 VRC01-resistant viruses (Table 1; also see Fig. S2 in the supplemental material). Among the viruses that were neutralized, VRC07 displayed ~2-fold higher potency than VRC01, with a geometric mean IC_{50} of 0.11 μg/ml (Fig. 1C; also see Fig. S2).

To understand VRC07 binding at the atomic level, we determined the crystal structure of VRC07 in complex with a clade A/E core gp120 (see Table S1 in the supplemental material). An overlay of the VRC07-gp120 structure with that of the VRC01-gp120 structure (20) revealed that these antibodies have the same modes of gp120 recognition (Fig. 1D). However, similar to what was described for NIH45-46 (48), the extended CDR H3 of VRC07 created new contacts between gp120 and residues R100a, D100b, and Y100c of VRC07 (Fig. 1D and E), doubling the CDR H3-mediated contact area relative to that of VRC01 (see Fig. S3 in the supplemental material).

Structure-guided optimizations improve the neutralization potency of VRC07 *in vitro*. Although VRC07 was potent in HIV-1 neutralization assays (see Fig. S2 in the supplemental material), we sought to engineer additional increases in neutralization potency and breadth (Fig. 2). Previously, Diskin et al. altered a single heavy-chain glycine residue to tryptophan (G54W) (68) to mimic the interaction between the phenylalanine (F43) of CD4 and a hydrophobic binding pocket region on gp120 (77). This modification increased the potency and breadth of NIH45-46 (68). Our structural studies on the clonal variant VRC03 also showed that

TABLE 1 Virus neutralization characteristics at IC_{50} and IC_{80}

Antibody	No. of viruses	No. (%) of viruses neutralized at:		Titer of:					
				Neutralized viruses[a]			All viruses[a]		
		<50 μg/ml	<1 μg/ml	Median	Geometric mean	Fold improvement from VRC01	Median	Geometric mean	Fold improvement from VRC01
		Value(s) determined at IC_{50}							
VRC01	179	159 (89)	138 (77)	0.23	0.221		0.297	0.434	
VRC07	179	166 (93)	149 (83)	0.119	0.114	1.9	0.129	0.187	2.3
VRC07-501-LS	179	171 (96)	164 (92)	0.05	0.041	5.4	0.052	0.058	7.5
VRC07-508-LS	179	168 (94)	159 (89)	0.04	0.043	5.1	0.051	0.069	6.3
VRC07-523-LS	179	171 (96)	165 (92)	0.046	0.039	5.6	0.047	0.055	7.9
VRC07-544-LS	179	170 (95)	162 (91)	0.058	0.05	4.4	0.065	0.073	5.9
		Value(s) determined at IC_{80}							
VRC01	179	156 (87)	78 (44)	1.013	0.98		1.3	1.775	
VRC07	179	164 (92)	122 (68)	0.41	0.414	2.4	0.462	0.656	2.7
VRC07-501-LS	179	169 (94)	154 (86)	0.193	0.16	6.1	0.208	0.229	7.7
VRC07-508-LS	179	165 (92)	146 (82)	0.188	0.178	5.5	0.211	0.291	6.1
VRC07-523-LS	179	170 (95)	152 (85)	0.229	0.197	5	0.242	0.269	6.6
VRC07-544-LS	179	169 (94)	146 (82)	0.236	0.209	4.7	0.269	0.292	6.1

[a] Median and geometric mean titers were calculated only for samples with an IC_{50} or IC_{80} of <50 μg/ml.
[b] Median and geometric mean titers were calculated for all viruses, and values of >50 μg/ml were set to 100 μg/ml.

position 54 contained a natural tryptophan that mimicked the gp120-$F43_{CD4}$ binding (26). Thus, we began by adding this tryptophan mutation to VRC07. Consistent with the observations for NIH45-46 (68), we observed an increase in binding to gp120 by ELISA and enhanced neutralization potency for VRC07-G54W (see Fig. S4a in the supplemental material). We crystallized the VRC07-G54W variant with an HIV-1 gp120 core and confirmed that the tryptophan residue increases the contact area with gp120 (see Fig. S4b). Unfortunately, the VRC07-G54W variant reacted positively in two assays of autoreactivity (73), antinuclear antibody staining of human epithelial (HEp-2) cells and binding to cardiolipin (Fig. 3).

To determine whether an alternative amino acid at position 54 could increase potency without increasing autoreactivity, we performed a comprehensive mutational analysis for position 54, testing all 20 amino acids (see Fig. S4 and Table S2 in the supplemental material). Many VRC07 variants with hydrophobic or positively charged amino acids at position 54 showed enhanced binding to gp120 (see Fig. S4a), but most of these substitutions also resulted in autoreactivity similar to that of the G54W mutation. However, the alteration of G54 to a histidine resulted in increased potency and breadth with minimal levels of autoreactivity (see Fig. S4c and d). Further, the crystal structure of VRC07-G54H with gp120 revealed that this histidine interacted with the target hydrophobic pocket in the gp120 CD4bs (Fig. 2A). Additional analysis of the interface between VRC07 and gp120 revealed that the N-terminal residues of the light chain of VRC07 were in close proximity to variable region 5 (V5) of gp120 and were disordered (Fig. 2A). This suggested that the N terminus of the light chain did not make critical contacts with gp120 and that the light chain encounters steric hindrance with V5. The V5 region often contains both sequence and length variations, suggesting that divergent HIV-1 strains with V5 insertions also could clash with the VRC07 light-chain N terminus. Therefore, we generated antibody variants with modifications of the four most N-terminal residues of the VRC07 light chain. These variants included amino acid deletions, changes to amino acids with smaller side chains, and combinations of both (see Fig. S5 and Table S2 in the supplemental material). Most of the deletions increased neutralization potency, but many also increased autoreactivity. A two-amino-acid deletion (E1 and I2) along with a change of the third residue from valine to serine (V3S) increased potency ~2.5-fold (~7-fold increase over that of VRC01) on a representative 20-virus neutralization panel without altering autoreactivity (see Fig. S5).

Additionally, we explored mutations that altered the heavy-chain–light-chain interface, the antibody-antigen interface, the hydrophobicity profile of the antibody, sites of N-linked glycosylation, and reversions to germ line residues (64) (see Table S2 in the supplemental material). From these analyses, we identified two sets of mutations to include in the lead-optimized candidates: framework region germ line reversions in the heavy chain (mutations I37V/T93A) and a combination of five mutations in the light chain, named hpL02, designed to increase solubility (four hydrophobic to hydrophilic amino acid mutations on the surface of the antibody, namely, mutations I20T, W67S, V106Q, and I108N, plus a mutation to remove an N-linked glycosylation site, N72T) (Fig. 2c). Bjorkman and colleagues (48) identified a light chain mutation (S28Y) in NIH45-46-G54W that increases potency; however, a tyrosine was present already in this position in VRC07 (and VRC01).

From initial neutralization and autoreactivity screening assays, we selected four optimized candidates for detailed characterization (Fig. 2 and 3), including the assessment of autoreactivity and neutralization breadth and potency on a large panel of 179 viral strains (see Fig. S6 in the supplemental material). All four VRC07-optimized antibodies demonstrated increased breadth and potency compared to VRC01 and VRC07 (Fig. 2C; also see Fig. S6). These changes improved the overall breadth to 96% and, based on geometric mean IC_{50} and IC_{80} values, increased potency 4.4- to 7.9-fold compared to that of VRC01 (Table 1). VRC07-523, the most potent of the engineered variants, was 7.9-fold more potent than VRC01 on the basis of geometric mean IC_{50} titers (Table 1). VRC07-501 and VRC07-508 both displayed moderate autoreactivity (scoring

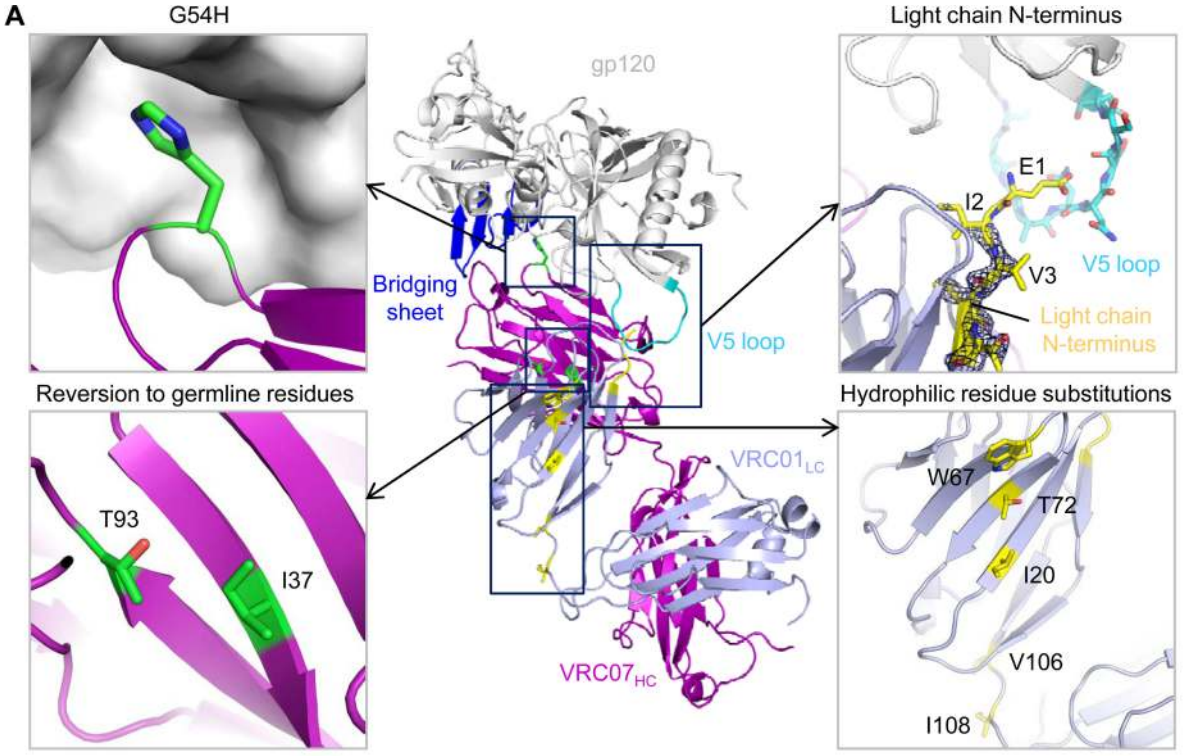

B

	Heavy chain modifications			Light chain modifications		
	Extended CDRH3	Framework germline (I37V, T93A)	G54H	E1/I2 deletion	V3S	Solubility mutations
VRC01						
VRC07	✓					
VRC07-501	✓		✓	✓		
VRC07-508	✓	✓	✓	✓		✓
VRC07-523	✓		✓	✓	✓	
VRC07-544	✓	✓	✓	✓	✓	

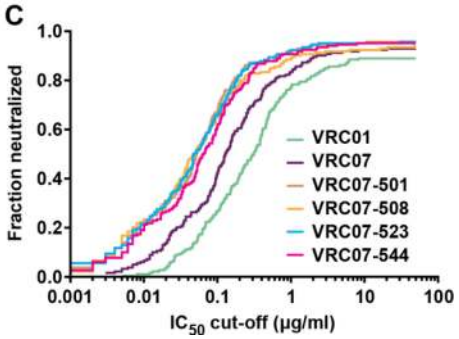

FIG 2 Structure-guided optimizations of VRC07 increase potency and breadth. (A) The structure of VRC07 (heavy chain, purple; light chain, light purple) bound to gp120 (gray; bridging sheet, blue; V5 loop, cyan). The insets show the series of mutations that were engineered into VRC07 to increase neutralization potency and breadth while maintaining minimal autoreactivity. Top left, alteration of the heavy-chain G54 to H increases binding to gp120 (gray) by mimicking the $F43_{CD4}$ binding to gp120. The crystal structure confirmed that the VRC07–G54H MAb and gp120 interaction resembles the CD4-gp120 interaction. Top right, modification of the N terminus of the light chain. Poor resolution (shown by a lack of electron density [dark blue mesh]) in the crystal structure of the N-terminal end of the VRC07 light chain suggests that this region is disordered. Modeling the N-terminal residues (yellow) reveals a potential clash with the V5 loop (cyan). Deletion of light-chain residues E1 and I2 along with a V3S mutation minimized the potential clash with the V5 loop. Bottom left, two somatically mutated residues (I37 and T93, green) were reverted to their germ line amino acids (V and A, respectively), resulting in improved potency. Bottom right, replacement of selected hydrophobic residues (highlighted in yellow and labeled) in the light chain with hydrophilic residues were designed to enhance solubility and resulted in increased potency. An additional mutation (N72T) removed the N-linked glycosylation site in the light chain. (B) Mutations included in each of the optimized VRC07 MAb are summarized. (C) Antibodies were tested against a panel of 179 HIV-1 strains. The fraction of viruses neutralized at the given IC_{50} is shown. The optimized VRC07 variants (VRC07-501, VRC07-508, VRC07-523, and VRC07-544) were tested in an IgG1 format containing the FcRn binding site LS mutation. The constant region LS mutation has no effect on neutralization.

1+ on the HEp-2 assay when tested at a concentration of 25 μg/ml), although they were less autoreactive than VRC07-G54W (which scored 2+ at the same concentration), while VRC07-523 and VRC07-544 both had minimal autoreactivity (and scored negative when tested at 25 μg/ml) (Fig. 3).

Pharmacokinetics of VRC07 variants in nonhuman primates. We investigated the plasma half-life of the optimized VRC07 variants in Indian-origin rhesus macaques (Fig. 4A and D; also see Fig. S7a in the supplemental material). While the infusion of human antibodies into monkeys generally results in a shorter half-life (78) than the typical 21-day average half-life of IgG1 in humans (79), the NHP model often is used for comparative pharmacokinetic studies as a guide to the selection of agents for human testing. Published data suggested that antibody autoreactivity reduces circulating plasma half-life (80). Therefore, we first compared the pharmacokinetics of wild-type VRC07 to the highly autoreactive variant VRC07–G54W. Using standard measures of antibody plasma half-life, area under the curve, and clearance,

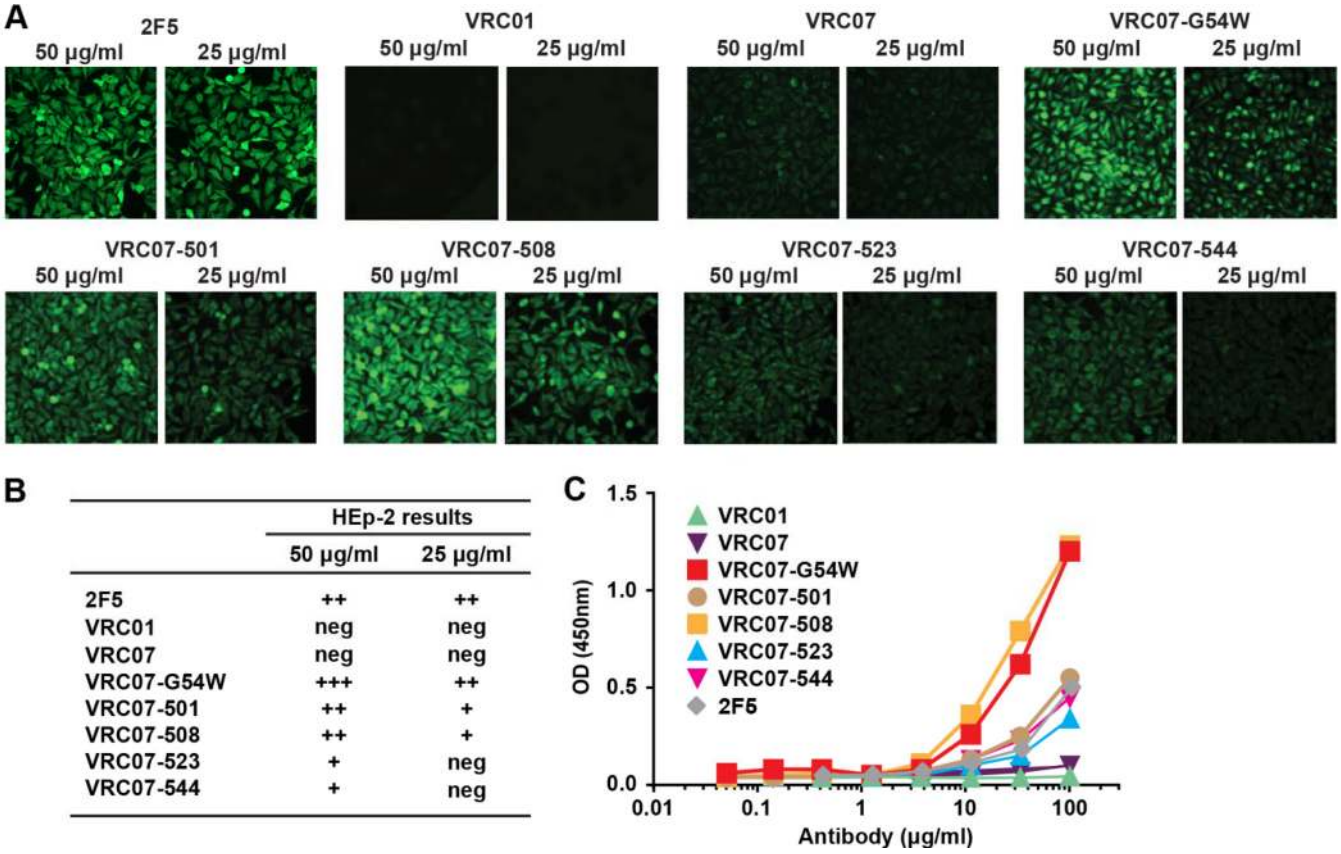

FIG 3 Autoreactivity of optimized VRC07 MAbs. (A) The reactivity of VRC07 variants to HEp-2 human epithelial cells was analyzed with an immunofluorescence cell staining assay. The autoreactive antibody 2F5 also was included in the analysis. Antibodies were tested at 50 μg/ml and 25 μg/ml, and scores are summarized in panel B. neg, negative. (C) MAb binding to cardiolipin, a mitochondrial membrane phospholipid, was assessed by ELISA. VRC07 variants and 2F5 were tested at 100 μg/ml and 3-fold serial dilutions. In both assays, the optimized VRC07 variants (VRC07-501, VRC07-508, VRC07-523, and VRC07-544) were tested in an IgG1 format containing the FcRn binding site LS mutation (described in the legend to Fig. 4). The constant region LS mutation does not affect autoreactivity results. OD, optical density.

VRC07-G54W displayed circulating levels ~2-fold lower than that of wild-type VRC07.

To improve the plasma half-life of VRC07, we incorporated a previously described set of two amino acid mutations (M428L/N434S; referred to as LS) that increase half-life by increasing affinity for the neonatal Fc-receptor (FcRn), which results in the recirculation of functional IgG (74, 78). The VRC07-LS mutant displayed a 2- to 3-fold increase in plasma half-life compared to wild-type VRC07 in rhesus macaques (Fig. 4B and D). Based on these data, the four optimized VRC07 variants were constructed with this LS mutation, and the pharmacokinetic properties of these antibodies were assessed *in vivo*. Among the four variants, VRC07-523-LS displayed a longer half-life (9.8 days) than the other three variants, close to the half-life of VRC07-LS (11.6 days). For all four optimized variants, the plasma MAb levels and half-lives in rhesus macaques were intermediate between that of VRC07 and VRC07-LS (Fig. 4C and D). When MAb levels in rectal mucosal secretions were measured, antibody VRC07-523-LS was detectable for at least 14 days (see Fig. S7b in the supplemental material).

Optimized VRC07 protects against infection at lower plasma concentrations. To determine if an antibody with increased neutralization potency *in vitro* would confer greater *in vivo* protection, we compared the ability of VRC01-LS and VRC07-523-LS to protect rhesus macaques from intrarectal challenge with SHIV BaLP4. We assessed the neutralization sensitivity of the SHIV BaLP4 challenge stock to both antibodies. VRC07-523-LS neutralized SHIV BaLP4 at a 5.6-fold lower concentration than VRC01 (IC_{50}s of 0.005 μg/ml and 0.028 μg/ml, respectively) (Fig. 5A and B). Challenge experiments were designed using varied antibody infusion doses to allow a calculation of the plasma MAb concentration that provides 50% protection (plasma EC_{50}). MAbs were administered intravenously, and animals were challenged mucosally 5 days later. This approach allowed us to compare the effective plasma concentration of VRC07-523-LS and VRC01-LS at the time of SHIV challenge irrespective of the infusion dose. When VRC07-523-LS was administered at doses of 0.2 mg/kg and 0.05 mg/kg, 3 of 4 animals and 0 of 4 animals were protected, respectively. For VRC01-LS, 5 of 12 animals were protected at a dose of 0.3 mg/kg (Fig. 5C; also see Fig. S8 in the supplemental material). We measured plasma antibody levels at the time of SHIV challenge and used a binary (probit) regression model to calculate the EC_{50}s: the EC_{50} titers for VRC07-523-LS and VRC01-LS were 0.47 μg/ml and 2.5 μg/ml, respectively, and the 90% confidence intervals for these values did not overlap (Fig. 5D). This difference in the regression curves for VRC01-LS and VRC07-23-LS trended

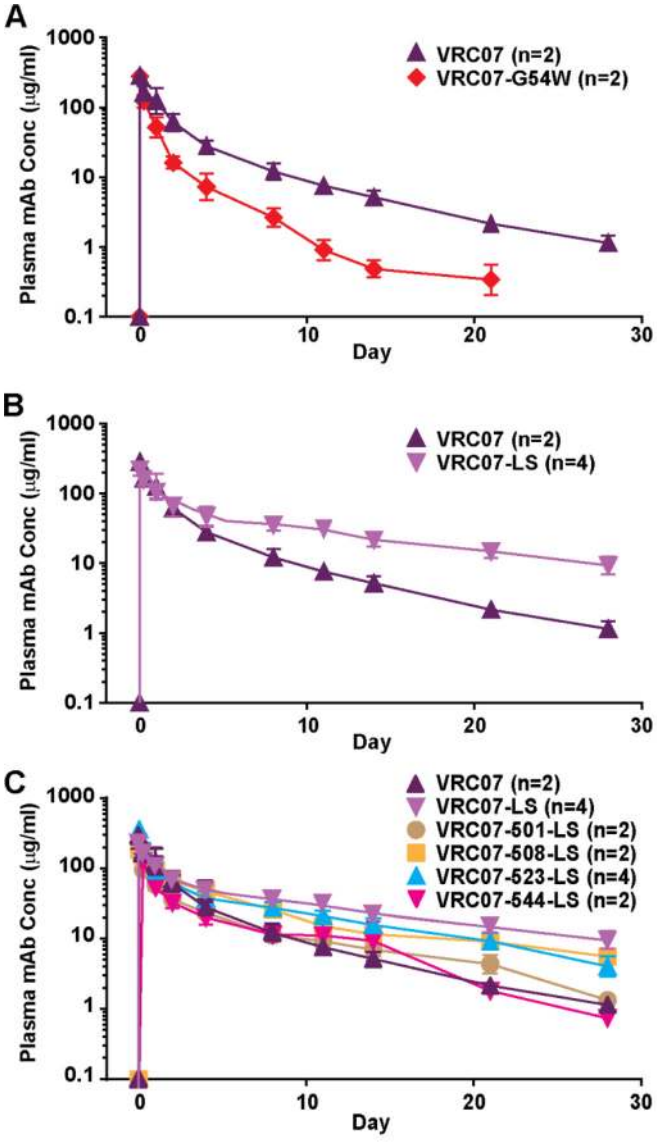

D

	Number of NHP	Half-life (days)	Area under curve (day*ug/ml)	Clearance (ml/day/kg)
VRC07	n=2	4.9	452.4	22.6
VRC07-G54W	n=4	3.8	228.8	44.9
VRC07-LS	n=2	11.6	877.0	8.9
VRC07-501-LS	n=2	6.8	236.5	38.7
VRC07-508-LS	n=2	7.0	456.4	20.3
VRC07-523-LS	n=4	9.8	886.5	10.1
VRC07-544-LS	n=2	8.1	397.4	23.4

FIG 4 Optimized VRC07 MAbs with the LS mutation have extended plasma half-lives. Pharmacokinetic studies were performed in male rhesus macaques. All MAbs were administered at 10 mg/kg intravenously, and plasma levels were monitored by a gp120 core (RSC3) ELISA. The number of NHPs is indicated, and means ± standard deviations are plotted. (A) The pharmacokinetics of VRC07 and VRC07-G54W are shown. (B) An FcRn binding site mutation (LS) was added to VRC07 and improved plasma half-life by ~2-fold. (C) VRC07-508-LS and VRC07-523-LS also had increased plasma levels and extended half-lives compared to wild-type VRC07, while VRC07-501-LS and VRC07-544-LS had pharmacokinetics similar to those of VRC07. (D) Terminal (β) phase half-life was calculated through day 21 using a noncompartmental model. Mean areas under the curve and clearance rates also are shown for each MAb. All calculations were performed with WinNonlin software (Pharsight).

toward significance ($P = 0.07$). Therefore, optimized antibody showed a >5-fold increase in potency compared to the parental antibody, consistent with its ability to better neutralize virus *in vitro*. No significant difference in peak viral loads or time to viremia was observed between any of the treatment groups.

DISCUSSION

Growing evidence in animal model studies suggests that potent HIV-1 MAbs can prevent infection (11, 42–44) or reduce viremia during chronic infection (45, 46, 81). These successes have renewed interest in testing MAbs in clinical trials (13, 82, 83). The overall efficacy of an HIV-1 MAb likely depends on several characteristics, including the breadth of reactivity (i.e., the fraction of circulating virus strains neutralized), the neutralization potency (i.e., the concentration of antibody needed to prevent infection), and the pharmacokinetic properties (e.g., circulating half-life and tissue localization). Here, we sought to improve the potency and breadth of antibody VRC01 and used the resulting antibody to demonstrate a relationship between *in vitro* neutralization potency and *in vivo* efficacy. Additionally, we improved the half-life both by minimizing autoreactivity and by adding Fc-region mutations that increase circulating plasma MAb levels. Thus, our lead candidate, VRC07-523-LS, was engineered to have *in vitro* and *in vivo* characteristics likely to increase clinical protective efficacy.

Our studies started with the well-characterized MAb VRC01, which has high *in vitro* potency and breadth and currently is being evaluated in phase I clinical trials. Using deep sequencing and bioinformatics, we identified a heavy-chain VRC01 clonal variant from donor 45 with moderately improved potency and breadth. Structure-based analyses were used to design variants with improved neutralization activity. Numerous mutations were explored, and mutations focused on the heavy-chain G54 residue and the N terminus of the light chain were found to have the most favorable *in vitro* characteristics. In combination, a G54H point mutation on the heavy chain, a deletion of the two N-terminal light-chain amino acids (E1 and I2), and a V3S point mutation on the light chain led to a 5- to 8-fold increase in neutralization potency (based on geometric mean IC_{50} and IC_{80} values) and improved breadth (93% for VRC07 to 96% for VRC07-523).

Notably, these mutations improved potency without causing substantial autoreactivity. This feature was particularly important because autoreactivity and off-target binding may decrease plasma MAb levels and promote unwanted immunopathology. For example, in human clinical trials, the infusion of a combination of the gp41 MAbs 4E10 and 2F5, which are both autoreactive (73), and 2G12, which is not autoreactive, was associated with a prolonged *in vitro* blood-clotting time (partial thromboplastin time) (84). In the same studies, MAbs 4E10 and 2F5 both had shorter half-lives than the nonautoreactive MAb 2G12 (73, 84–86). Additionally, during the development of motavizumab, a second-generation anti-RSV MAb, autoreactivity (broad tissue binding and cross-reactivity) also was associated with lower circulating plasma levels (87).

To compare pharmacokinetic properties, including circulating plasma half-life, VRC07 variants were analyzed in rhesus ma-

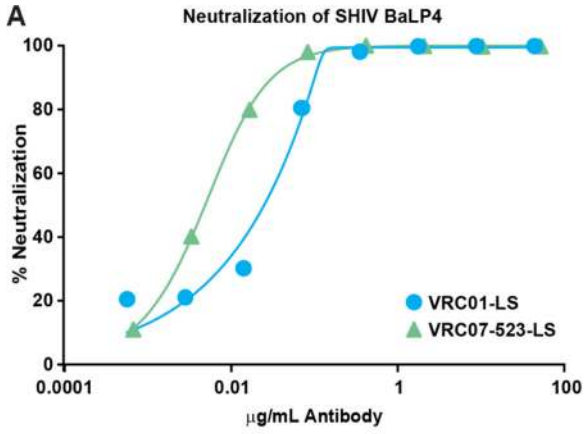

B

	SHIV-BaL	
	IC_{50} (μg/mL)	IC_{80} (μg/mL)
VRC01-LS	0.028	0.069
VRC07-523-LS	0.005	0.016
Fold more potent	5.6	4.3

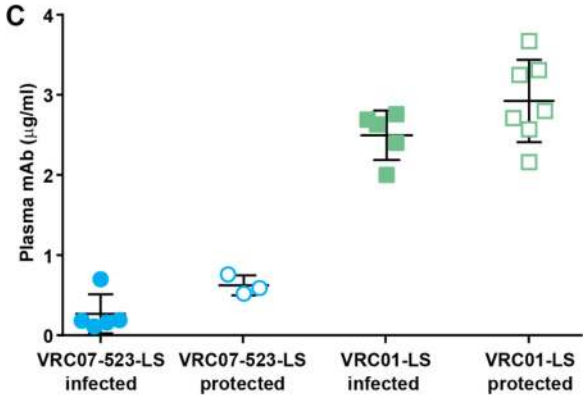

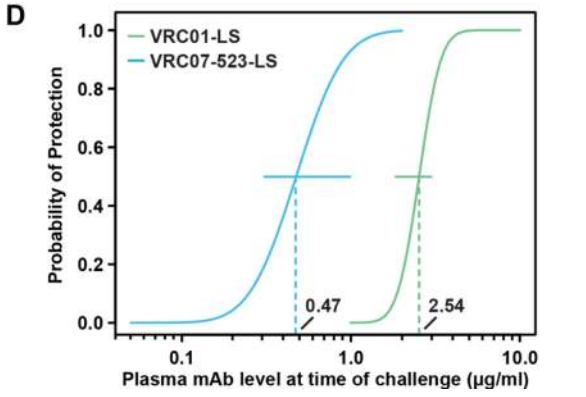

FIG 5 Improved protective efficacy of VRC07-523-LS compared to VRC01-LS. (A) Neutralization assays were performed with the SHIV-BaLP4 challenge stock and antibody VRC01-LS or VRC07-523-LS using TZM-bl target cells. (B) VRC07-523-LS is about 5-fold more potent than VRC01-LS against the SHIV-BaLP4 stock *in vitro*. (C) Rhesus macaques were administered either 0.2 mg/kg or 0.05 mg/kg of VRC07-523-LS ($n = 4$ each) or 0.3 mg/kg of VRC01-LS ($n = 12$) and challenged intrarectally with SHIV-BaLP4 5 days later. Plasma concentrations of VRC07-523-LS and VRC01-LS at the time of challenge were determined by RSC3 ELISA. Plasma MAb levels of animals that became infected are graphed with closed icons, and plasma levels of animals that were protected are graphed with open icons. (D) The probability of protection from SHIV challenge can be predicted using a probit regression model based on the plasma MAb concentration at the time of challenge. Curves for VRC01-LS (green) and VRC07-523-LS (blue) graph the calculated probability of protection (*y* axis) at increasing plasma MAb levels (*x* axis). The EC_{50} for VRC07-523-LS was 0.47 μg/ml (90% confidence interval [CI], 0.31 to 0.96 μg/ml), and the VRC01-LS EC_{50} was 2.54 μg/ml (90% CI, 1.86 to 2.96 μg/ml). Ninety percent confidence intervals are shown for each curve with horizontal lines, and these do not overlap.

caques. These experiments confirmed that the autoreactive MAb VRC07-G54W had a shorter half-life than VRC07. These *in vivo* data suggested an association between antibody autoreactivity and shorter half-life and provided further rationale for pursuing VRC07 variants with the heavy-chain G54H mutation that showed low levels of autoreactivity. We constructed the optimized VRC07 variants (VRC07-501, VRC07-508, VRC07-523, and VRC07-544) with a two-amino-acid LS mutation in the IgG Fc region that has been shown to increase affinity for FcRn and to increase antibody half-life *in vivo* (78). We recently demonstrated that MAb VRC01-LS, with enhanced FcRn binding, displayed increased gut mucosal tissue localization, which improved protection against SHIV infection in the NHP model (74). Our preferred variant, VRC07-523-LS, displayed a >2-fold improved half-life compared to that of the wild-type VRC07 without the LS mutation.

In vitro neutralization often is assumed to be the most important predictive factor in protection against *in vivo* lentiviral infection; however, some studies have suggested a role of Fc-mediated effector functions, such as antibody-dependent cellular cytotoxicity (ADCC), in protection (88, 89). Of note, the LS mutations introduced into the CH3 domain do not affect ADCC activity (74, 78). While we did not address the role of ADCC here, we were able to directly address the relationship of *in vitro* neutralization potency and *in vivo* efficacy. Thus, we compared the ability of VRC01-LS and the optimized VRC07-523-LS to protect NHPs from mucosal SHIV challenge. VRC01-LS and VRC07-523-LS were administered at low doses to monkeys that then were challenged with SHIV BaLP4. VRC07-523-LS was able to protect at levels 5 times lower than that of VRC01-LS. Although the differences in protection were slightly above the threshold for statistical significance, we believe our results strongly suggest a relationship between *in vitro* and *in vivo* potency. Notably, the ~5-fold difference in protection was comparable to that seen in neutralization assays *in vitro*.

In summary, we show that a process of iterative structure-based design and *in vitro* analyses improved the neutralization activity of VRC01, a MAb that targets the CD4bs of the HIV-1 envelope glycoprotein gp120. VRC01 is able to neutralize 89% of HIV-1 strains with a geometric mean IC_{50} of 0.22 μg/ml. The optimized VRC07-523 neutralized 96% of HIV-1 strains and was 5- to 8-fold more potent than VRC01. This improvement in potency *in vitro* correlated with increased protective efficacy against SHIV challenge *in vivo*. Importantly, VRC07-523 displayed minimal autoreactivity, and its half-life was further extended with the addition of the LS mutations in the FcRn binding site. These *in vitro* and preclinical data suggest that it is possible to improve the efficacy of naturally occurring broadly neutralizing HIV-1 antibodies and that this approach could be applied to other anti-HIV-1 antibodies. Therefore, these modifications optimize bio-

logical properties of such anti-HIV-1 broadly neutralizing antibodies that will increase the likelihood for protection against HIV-1 infection in humans.

ACKNOWLEDGMENTS

We thank members of the Structural Biology Section, Structural Bioinformatics Core Section, Humoral Immunology Section, Virology Laboratory, Vaccine Production Program, and Vaccine Translational Research Program of the Vaccine Research Center, NIAID, for advice and technical support, and Brenda Hartman for assistance with figure preparation. We thank J. Baalwa, D. Ellenberger, F. Gao, B. Hahn, K. Hong, J. Kim, F. McCutchan, D. Montefiori, L. Morris, J. Overbaugh, E. Sanders-Buell, G. Shaw, R. Swanstrom, M. Thomson, S. Tovanabutra, C. Williamson, and L. Zhang for contributing the HIV-1 Envelope plasmids used in our neutralization panel. We thank B. Barnabas, R. Blakesley, G. Bouffard, S. Brooks, H. Coleman, M. Dekhtyar, M. Gregory, X. Guan, J. Gupta, J. Han, S. Ho, R. Legaspi, Q. Maduro, C. Masiello, B. Maskeri, J. McDowell, C. Montemayor, M. Park, N. Riebow, K. Schandler, B. Schmidt, C. Sison, M. Stantripop, J. Thomas, P. Thomas, M. Vemulapalli and A. Young for assistance with 454 pyrosequencing at NISC.

Support for this work was provided by the Intramural Research Program of the VRC, NIAID, NIH. Additionally, this research has been supported in part by a grant from the Foundation for the National Institutes of Health with support from the Collaboration for AIDS Vaccine Discovery (CAVD) award OPP1039775 from the Bill & Melinda Gates Foundation. B.R.D. and K.E.R. were supported by NIH grant R01 GM78031 (to B.R.D.).

Use of sector 22 (Southeast Region Collaborative Access team) at the Advanced Photon Source was supported by the U.S. Department of Energy, Basic Energy Sciences, Office of Science, under contract number W-31-109-Eng-38.

We declare that an intellectual property application has been filed by NIH based on data presented in this paper.

REFERENCES

1. **Plotkin SA.** 2008. Vaccines: correlates of vaccine-induced immunity. Clin. Infect. Dis. **47:**401–409. http://dx.doi.org/10.1086/589862.
2. **Koff WC, Burton DR, Johnson PR, Walker BD, King CR, Nabel GJ, Ahmed R, Bhan MK, Plotkin SA.** 2013. Accelerating next-generation vaccine development for global disease prevention. Science **340:**1232910. http://dx.doi.org/10.1126/science.1232910.
3. **Mascola JR, Lewis MG, Stiegler G, Harris D, VanCott TC, Hayes D, Louder MK, Brown CR, Sapan CV, Frankel SS, Lu Y, Robb ML, Katinger H, Birx DL.** 1999. Protection of macaques against pathogenic simian/human immunodeficiency virus 89.6PD by passive transfer of neutralizing antibodies. J. Virol. **73:**4009–4018.
4. **Mascola JR, Stiegler G, VanCott TC, Katinger H, Carpenter CB, Hanson CE, Beary H, Hayes D, Frankel SS, Birx DL, Lewis MG.** 2000. Protection of macaques against vaginal transmission of a pathogenic HIV-1/SIV chimeric virus by passive infusion of neutralizing antibodies. Nat. Med. **6:**207–210. http://dx.doi.org/10.1038/72318.
5. **Parren PW, Marx PA, Hessell AJ, Luckay A, Harouse J, Cheng-Mayer C, Moore JP, Burton DR.** 2001. Antibody protects macaques against vaginal challenge with a pathogenic R5 simian/human immunodeficiency virus at serum levels giving complete neutralization in vitro. J. Virol. **75:**8340–8347. http://dx.doi.org/10.1128/JVI.75.17.8340-8347.2001.
6. **Nishimura Y, Igarashi T, Haigwood NL, Sadjadpour R, Donau OK, Buckler C, Plishka RJ, Buckler-White A, Martin MA.** 2003. Transfer of neutralizing IgG to macaques 6 h but not 24 h after SHIV infection confers sterilizing protection: implications for HIV-1 vaccine development. Proc. Natl. Acad. Sci. U. S. A. **100:**15131–15136. http://dx.doi.org/10.1073/pnas.2436476100.
7. **Veazey RS, Shattock RJ, Pope M, Kirijan JC, Jones J, Hu Q, Ketas T, Marx PA, Klasse PJ, Burton DR, Moore JP.** 2003. Prevention of virus transmission to macaque monkeys by a vaginally applied monoclonal antibody to HIV-1 gp120. Nat. Med. **9:**343–346. http://dx.doi.org/10.1038/nm833.
8. **Hessell AJ, Poignard P, Hunter M, Hangartner L, Tehrani DM, Bleeker WK, Parren PW, Marx PA, Burton DR.** 2009. Effective, low-titer antibody protection against low-dose repeated mucosal SHIV challenge in macaques. Nat. Med. **15:**951–954. http://dx.doi.org/10.1038/nm.1974.
9. **Hessell AJ, Rakasz EG, Poignard P, Hangartner L, Landucci G, Forthal DN, Koff WC, Watkins DI, Burton DR.** 2009. Broadly neutralizing human anti-HIV antibody 2G12 is effective in protection against mucosal SHIV challenge even at low serum neutralizing titers. PLoS Pathog. **5:**e1000433. http://dx.doi.org/10.1371/journal.ppat.1000433.
10. **Hessell AJ, Rakasz EG, Tehrani DM, Huber M, Weisgrau KL, Landucci G, Forthal DN, Koff WC, Poignard P, Watkins DI, Burton DR.** 2010. Broadly neutralizing monoclonal antibodies 2F5 and 4E10 directed against the human immunodeficiency virus type 1 gp41 membrane-proximal external region protect against mucosal challenge by simian-human immunodeficiency virus SHIVBa-L. J. Virol. **84:**1302–1313. http://dx.doi.org/10.1128/JVI.01272-09.
11. **Moldt B, Rakasz EG, Schultz N, Chan-Hui PY, Swiderek K, Weisgrau KL, Piaskowski SM, Bergman Z, Watkins DI, Poignard P, Burton DR.** 2012. Highly potent HIV-specific antibody neutralization in vitro translates into effective protection against mucosal SHIV challenge in vivo. Proc. Natl. Acad. Sci. U. S. A. **109:**18921–18925. http://dx.doi.org/10.1073/pnas.1214785109.
12. **Burton DR, Ahmed R, Barouch DH, Butera ST, Crotty S, Godzik A, Kaufmann DE, McElrath MJ, Nussenzweig MC, Pulendran B, Scanlan CN, Schief WR, Silvestri G, Streeck H, Walker BD, Walker LM, Ward AB, Wilson IA, Wyatt R.** 2012. A blueprint for HIV vaccine discovery. Cell Host Microbe **12:**396–407. http://dx.doi.org/10.1016/j.chom.2012.09.008.
13. **Kwong PD, Mascola JR, Nabel GJ.** 2013. Broadly neutralizing antibodies and the search for an HIV-1 vaccine: the end of the beginning. Nat. Rev. Immunol. **13:**693–701. http://dx.doi.org/10.1038/nri3516.
14. **Kwong PD, Mascola JR.** 2012. Human antibodies that neutralize HIV-1: identification, structures, and B cell ontogenies. Immunity **37:**412–425. http://dx.doi.org/10.1016/j.immuni.2012.08.012.
15. **Walker LM, Phogat SK, Chan-Hui PY, Wagner D, Phung P, Goss JL, Wrin T, Simek MD, Fling S, Mitcham JL, Lehrman JK, Priddy FH, Olsen OA, Frey SM, Hammond PW, Kaminsky S, Zamb T, Moyle M, Koff WC, Poignard P, Burton DR.** 2009. Broad and potent neutralizing antibodies from an African donor reveal a new HIV-1 vaccine target. Science **326:**285–289. http://dx.doi.org/10.1126/science.1178746.
16. **Corti D, Langedijk JP, Hinz A, Seaman MS, Vanzetta F, Fernandez-Rodriguez BM, Silacci C, Pinna D, Jarrossay D, Balla-Jhagjhoorsingh S, Willems B, Zekveld MJ, Dreja H, O'Sullivan E, Pade C, Orkin C, Jeffs SA, Montefiori DC, Davis D, Weissenhorn W, McKnight A, Heeney JL, Sallusto F, Sattentau QJ, Weiss RA, Lanzavecchia A.** 2010. Analysis of memory B cell responses and isolation of novel monoclonal antibodies with neutralizing breadth from HIV-1-infected individuals. PLoS One **5:**e8805. http://dx.doi.org/10.1371/journal.pone.0008805.
17. **Pancera M, McLellan JS, Wu X, Zhu J, Changela A, Schmidt SD, Yang Y, Zhou T, Phogat S, Mascola JR, Kwong PD.** 2010. Crystal structure of PG16 and chimeric dissection with somatically related PG9: structure-function analysis of two quaternary-specific antibodies that effectively neutralize HIV-1. J. Virol. **84:**8098–8110. http://dx.doi.org/10.1128/JVI.00966-10.
18. **Pejchal R, Walker LM, Stanfield RL, Phogat SK, Koff WC, Poignard P, Burton DR, Wilson IA.** 2010. Structure and function of broadly reactive antibody PG16 reveal an H3 subdomain that mediates potent neutralization of HIV-1. Proc. Natl. Acad. Sci. U. S. A. **107:**11483–11488. http://dx.doi.org/10.1073/pnas.1004600107.
19. **Wu X, Yang ZY, Li Y, Hogerkorp CM, Schief WR, Seaman MS, Zhou T, Schmidt SD, Wu L, Xu L, Longo NS, McKee K, O'Dell S, Louder MK, Wycuff DL, Feng Y, Nason M, Doria-Rose N, Connors M, Kwong PD, Roederer M, Wyatt RT, Nabel GJ, Mascola JR.** 2010. Rational design of envelope identifies broadly neutralizing human monoclonal antibodies to HIV-1. Science **329:**856–861. http://dx.doi.org/10.1126/science.1187659.
20. **Zhou T, Georgiev I, Wu X, Yang ZY, Dai K, Finzi A, Do Kwon Y, Scheid J, Shi W, Xu L, Yang Y, Zhu J, Nussenzweig MC, Sodroski J, Shapiro L, Nabel GJ, Mascola JR, Kwong PD.** 2010. Structural basis for broad and potent neutralization of HIV-1 by antibody VRC01. Science **329:**811–817. http://dx.doi.org/10.1126/science.1192819.
21. **Bonsignori M, Hwang KK, Chen X, Tsao CY, Morris L, Gray E, Marshall DJ, Crump JA, Kapiga SH, Sam NE, Sinangil F, Pancera M, Yongping Y, Zhang B, Zhu J, Kwong PD, O'Dell S, Mascola JR, Wu L, Nabel GJ, Phogat S, Seaman MS, Whitesides JF, Moody MA, Kelsoe G,**

Yang X, Sodroski J, Shaw GM, Montefiori DC, Kepler TB, Tomaras GD, Alam SM, Liao HX, Haynes BF. 2011. Analysis of a clonal lineage of HIV-1 envelope V2/V3 conformational epitope-specific broadly neutralizing antibodies and their inferred unmutated common ancestors. J. Virol. **85:**9998–10009. http://dx.doi.org/10.1128/JVI.05045-11.

22. **McLellan JS, Pancera M, Carrico C, Gorman J, Julien JP, Khayat R, Louder R, Pejchal R, Sastry M, Dai K, O'Dell S, Patel N, Shahzad-ul Hussan S, Yang Y, Zhang B, Zhou T, Zhu J, Boyington JC, Chuang GY, Diwanji D, Georgiev I, Kwon YD, Lee D, Louder MK, Moquin S, Schmidt SD, Yang ZY, Bonsignori M, Crump JA, Kapiga SH, Sam NE, Haynes BF, Burton DR, Koff WC, Walker LM, Phogat S, Wyatt R, Orwenyo J, Wang LX, Arthos J, Bewley CA, Mascola JR, Nabel GJ, Schief WR, Ward AB, Wilson IA, Kwong PD.** 2011. Structure of HIV-1 gp120 V1/V2 domain with broadly neutralizing antibody PG9. Nature **480:**336–343. http://dx.doi.org/10.1038/nature10696.
23. **Pejchal R, Doores KJ, Walker LM, Khayat R, Huang PS, Wang SK, Stanfield RL, Julien JP, Ramos A, Crispin M, Depetris R, Katpally U, Marozsan A, Cupo A, Maloveste S, Liu Y, McBride R, Ito Y, Sanders RW, Ogohara C, Paulson JC, Feizi T, Scanlan CN, Wong CH, Moore JP, Olson WC, Ward AB, Poignard P, Schief WR, Burton DR, Wilson IA.** 2011. A potent and broad neutralizing antibody recognizes and penetrates the HIV glycan shield. Science **334:**1097–1103. http://dx.doi.org/10.1126/science.1213256.
24. **Scheid JF, Mouquet H, Ueberheide B, Diskin R, Klein F, Oliveira TY, Pietzsch J, Fenyo D, Abadir A, Velinzon K, Hurley A, Myung S, Boulad F, Poignard P, Burton DR, Pereyra F, Ho DD, Walker BD, Seaman MS, Bjorkman PJ, Chait BT, Nussenzweig MC.** 2011. Sequence and structural convergence of broad and potent HIV antibodies that mimic CD4 binding. Science **333:**1633–1637. http://dx.doi.org/10.1126/science.1207227.
25. **Walker LM, Huber M, Doores KJ, Falkowska E, Pejchal R, Julien JP, Wang SK, Ramos A, Chan-Hui PY, Moyle M, Mitcham JL, Hammond PW, Olsen OA, Phung P, Fling S, Wong CH, Phogat S, Wrin T, Simek MD, Koff WC, Wilson IA, Burton DR, Poignard P.** 2011. Broad neutralization coverage of HIV by multiple highly potent antibodies. Nature **477:**466–470. http://dx.doi.org/10.1038/nature10373.
26. **Wu X, Zhou T, Zhu J, Zhang B, Georgiev I, Wang C, Chen X, Longo NS, Louder M, McKee K, O'Dell S, Perfetto S, Schmidt SD, Shi W, Wu L, Yang Y, Yang ZY, Yang Z, Zhang Z, Bonsignori M, Crump JA, Kapiga SH, Sam NE, Haynes BF, Simek M, Burton DR, Koff WC, Doria-Rose NA, Connors M, Mullikin JC, Nabel GJ, Roederer M, Shapiro L, Kwong PD, Mascola JR.** 2011. Focused evolution of HIV-1 neutralizing antibodies revealed by structures and deep sequencing. Science **333:**1593–1602. http://dx.doi.org/10.1126/science.1207532.
27. **Huang J, Ofek G, Laub L, Louder MK, Doria-Rose NA, Longo NS, Imamichi H, Bailer RT, Chakrabarti B, Sharma SK, Alam SM, Wang T, Yang Y, Zhang B, Migueles SA, Wyatt R, Haynes BF, Kwong PD, Mascola JR, Connors M.** 2012. Broad and potent neutralization of HIV-1 by a gp41-specific human antibody. Nature **491:**406–412. http://dx.doi.org/10.1038/nature11544.
28. **Mouquet H, Scharf L, Euler Z, Liu Y, Eden C, Scheid JF, Halper-Stromberg A, Gnanapragasam PN, Spencer DI, Seaman MS, Schuitemaker H, Feizi T, Nussenzweig MC, Bjorkman PJ.** 2012. Complex-type N-glycan recognition by potent broadly neutralizing HIV antibodies. Proc. Natl. Acad. Sci. U. S. A. **109:**E3268–E3277. http://dx.doi.org/10.1073/pnas.1217207109.
29. **Julien JP, Lee JH, Cupo A, Murin CD, Derking R, Hoffenberg S, Caulfield MJ, King CR, Marozsan AJ, Klasse PJ, Sanders RW, Moore JP, Wilson IA, Ward AB.** 2013. Asymmetric recognition of the HIV-1 trimer by broadly neutralizing antibody PG9. Proc. Natl. Acad. Sci. U. S. A. **110:**4351–4356. http://dx.doi.org/10.1073/pnas.1217537110.
30. **Julien JP, Sok D, Khayat R, Lee JH, Doores KJ, Walker LM, Ramos A, Diwanji DC, Pejchal R, Cupo A, Katpally U, Depetris RS, Stanfield RL, McBride R, Marozsan AJ, Paulson JC, Sanders RW, Moore JP, Burton DR, Poignard P, Ward AB, Wilson IA.** 2013. Broadly neutralizing antibody PGT121 allosterically modulates CD4 binding via recognition of the HIV-1 gp120 V3 base and multiple surrounding glycans. PLoS Pathog. **9:**e1003342. http://dx.doi.org/10.1371/journal.ppat.1003342.
31. **Kong L, Lee JH, Doores KJ, Murin CD, Julien JP, McBride R, Liu Y, Marozsan A, Cupo A, Klasse PJ, Hoffenberg S, Caulfield M, King CR, Hua Y, Le KM, Khayat R, Deller MC, Clayton T, Tien H, Feizi T, Sanders RW, Paulson JC, Moore JP, Stanfield RL, Burton DR, Ward AB, Wilson IA.** 2013. Supersite of immune vulnerability on the glycosylated face of HIV-1 envelope glycoprotein gp120. Nat. Struct. Mol. Biol. **20:**796–803. http://dx.doi.org/10.1038/nsmb.2594.
32. **Liao HX, Lynch R, Zhou T, Gao F, Alam SM, Boyd SD, Fire AZ, Roskin KM, Schramm CA, Zhang Z, Zhu J, Shapiro L, NCS Program, Mullikin JC, Gnanakaran S, Hraber P, Wiehe K, Kelsoe G, Yang G, Xia SM, Montefiori DC, Parks R, Lloyd KE, Scearce RM, Soderberg KA, Cohen M, Kamanga G, Louder MK, Tran LM, Chen Y, Cai F, Chen S, Moquin S, Du X, Joyce MG, Srivatsan S, Zhang B, Zheng A, Shaw GM, Hahn BH, Kepler TB, Korber BT, Kwong PD, Mascola JR, Haynes BF.** 2013. Co-evolution of a broadly neutralizing HIV-1 antibody and founder virus. Nature **496:**469–476. http://dx.doi.org/10.1038/nature12053.
33. **Pancera M, Shahzad-Ul-Hussan S, Doria-Rose NA, McLellan JS, Bailer RT, Dai K, Loesgen S, Louder MK, Staupe RP, Yang Y, Zhang B, Parks R, Eudailey J, Lloyd KE, Blinn J, Alam SM, Haynes BF, Amin MN, Wang LX, Burton DR, Koff WC, Nabel GJ, Mascola JR, Bewley CA, Kwong PD.** 2013. Structural basis for diverse N-glycan recognition by HIV-1-neutralizing V1-V2-directed antibody PG16. Nat. Struct. Mol. Biol. **20:**804–813. http://dx.doi.org/10.1038/nsmb.2600.
34. **Zhou T, Zhu J, Wu X, Moquin S, Zhang B, Acharya P, Georgiev IS, Altae-Tran HR, Chuang GY, Joyce MG, Do Kwon Y, Longo NS, Louder MK, Luongo T, McKee K, Schramm CA, Skinner J, Yang Y, Yang Z, Zhang Z, Zheng A, Bonsignori M, Haynes BF, Scheid JF, Nussenzweig MC, Simek M, Burton DR, Koff WC, NCS Program, Mullikin JC, Connors M, Shapiro L, Nabel GJ, Mascola JR, Kwong PD.** 2013. Multidonor analysis reveals structural elements, genetic determinants, and maturation pathway for HIV-1 neutralization by VRC01-class antibodies. Immunity **39:**245–258. http://dx.doi.org/10.1016/j.immuni.2013.04.012.
35. **Blattner C, Lee JH, Sliepen K, Derking R, Falkowska E, de la Pena AT, Cupo A, Julien JP, van Gils M, Lee PS, Peng W, Paulson JC, Poignard P, Burton DR, Moore JP, Sanders RW, Wilson IA, Ward AB.** 2014. Structural delineation of a quaternary, cleavage-dependent epitope at the gp41-gp120 interface on intact HIV-1 Env trimers. Immunity **40:**669–680. http://dx.doi.org/10.1016/j.immuni.2014.04.008.
36. **Scharf L, Scheid JF, Lee JH, West AP, Jr, Chen C, Gao H, Gnanapragasam PN, Mares R, Seaman MS, Ward AB, Nussenzweig MC, Bjorkman PJ.** 2014. Antibody 8ANC195 reveals a site of broad vulnerability on the HIV-1 envelope spike. Cell Rep. **7:**785–795. http://dx.doi.org/10.1016/j.celrep.2014.04.001.
37. **Huang J, Kang B, Pancera M, Lee JH, Tong T, Feng Y, Georgiev I, Chuang GY, Druz A, Doria-Rose NA, Laub L, Sliepen K, van Gils M, de la Peña AT, Derking R, Klasse PJ, Migueles SA, Bailer RT, Alam SM, Pugach P, Haynes BF, Wyatt RT, Sanders RW, Binley JM, Ward AB, Mascola JR, Kwong PD, Connors M.** 3 September 2014. Broad and potent HIV-1 neutralization by a human antibody that binds the gp41-120 interface. Nature http://dx.doi.org/10.1038/nature13601.
38. **Falkowska E, Le KM, Ramos A, Doores KJ, Lee JH, Blattner C, Ramirez A, Derking R, van Gils MJ, Liang CH, McBride R, von Bredow B, Shivatare SS, Wu CY, Chan-Hui PY, Liu Y, Feizi T, Zwick MB, Koff WC, Seaman MS, Swiderek K, Moore JP, Evans D, Paulson JC, Wong CH, Ward AB, Wilson IA, Sanders RW, Poignard P, Burton DR.** 2014. Broadly neutralizing HIV antibodies define a glycan-dependent epitope on the prefusion conformation of gp41 on cleaved envelope trimers. Immunity **40:**657–668. http://dx.doi.org/10.1016/j.immuni.2014.04.009.
39. **Falkowska E, Ramos A, Feng Y, Zhou T, Moquin S, Walker LM, Wu X, Seaman MS, Wrin T, Kwong PD, Wyatt RT, Mascola JR, Poignard P, Burton DR.** 2012. PGV04, an HIV-1 gp120 CD4 binding site antibody, is broad and potent in neutralization but does not induce conformational changes characteristic of CD4. J. Virol. **86:**4394–4403. http://dx.doi.org/10.1128/JVI.06973-11.
40. **West AP, Jr, Diskin R, Nussenzweig MC, Bjorkman PJ.** 2012. Structural basis for germ-line gene usage of a potent class of antibodies targeting the CD4-binding site of HIV-1 gp120. Proc. Natl. Acad. Sci. U. S. A. **109:**E2083–E2090. http://dx.doi.org/10.1073/pnas.1208984109.
41. **Pegu A, Yang ZY, Boyington JC, Wu L, Ko SY, Schmidt SD, McKee K, Kong WP, Shi W, Chen X, Todd JP, Letvin NL, Huang J, Nason MC, Hoxie JA, Kwong PD, Connors M, Rao SS, Mascola JR, Nabel GJ.** 2014. Neutralizing antibodies to HIV-1 envelope protect more effectively in vivo than those to the CD4 receptor. Sci. Transl. Med. **6:**243ra288. http://dx.doi.org/10.1126/scitranslmed.3008992.
42. **Veselinovic M, Neff CP, Mulder LR, Akkina R.** 2012. Topical gel formulation of broadly neutralizing anti-HIV-1 monoclonal antibody VRC01 confers protection against HIV-1 vaginal challenge in a human-

ized mouse model. Virology **432:**505–510. http://dx.doi.org/10.1016/j.virol.2012.06.025.
43. **Balazs AB, Chen J, Hong CM, Rao DS, Yang L, Baltimore D.** 2012. Antibody-based protection against HIV infection by vectored immunoprophylaxis. Nature **481:**81–84. http://dx.doi.org/10.1038/nature10660.
44. **Balazs AB, Ouyang Y, Hong CM, Chen J, Nguyen SM, Rao DS, An DS, Baltimore D.** 2014. Vectored immunoprophylaxis protects humanized mice from mucosal HIV transmission. Nat. Med. **20:**296–300. http://dx.doi.org/10.1038/nm.3471.
45. **Barouch DH, Whitney JB, Moldt B, Klein F, Oliveira TY, Liu J, Stephenson KE, Chang HW, Shekhar K, Gupta S, Nkolola JP, Seaman MS, Smith KM, Borducchi EN, Cabral C, Smith JY, Blackmore S, Sanisetty S, Perry JR, Beck M, Lewis MG, Rinaldi W, Chakraborty AK, Poignard P, Nussenzweig MC, Burton DR.** 2013. Therapeutic efficacy of potent neutralizing HIV-1-specific monoclonal antibodies in SHIV-infected rhesus monkeys. Nature **503:**224–228. http://dx.doi.org/10.1038/nature12744.
46. **Shingai M, Nishimura Y, Klein F, Mouquet H, Donau OK, Plishka R, Buckler-White A, Seaman M, Piatak M, Jr, Lifson JD, Dimitrov DS, Nussenzweig MC, Martin MA.** 2013. Antibody-mediated immunotherapy of macaques chronically infected with SHIV suppresses viraemia. Nature **503:**277–280. http://dx.doi.org/10.1038/nature12746.
47. **Klein F, Halper-Stromberg A, Horwitz JA, Gruell H, Scheid JF, Bournazos S, Mouquet H, Spatz LA, Diskin R, Abadir A, Zang T, Dorner M, Billerbeck E, Labitt RN, Gaebler C, Marcovecchio PM, Incesu RB, Eisenreich TR, Bieniasz PD, Seaman MS, Bjorkman PJ, Ravetch JV, Ploss A, Nussenzweig MC.** 2012. HIV therapy by a combination of broadly neutralizing antibodies in humanized mice. Nature **492:**118–122. http://dx.doi.org/10.1038/nature11604.
48. **Diskin R, Klein F, Horwitz JA, Halper-Stromberg A, Sather DN, Marcovecchio PM, Lee T, West AP, Jr, Gao H, Seaman MS, Stamatatos L, Nussenzweig MC, Bjorkman PJ.** 2013. Restricting HIV-1 pathways for escape using rationally designed anti-HIV-1 antibodies. J. Exp. Med. **210:**1235–1249. http://dx.doi.org/10.1084/jem.20130221.
49. **Shibata R, Igarashi T, Haigwood N, Buckler-White A, Ogert R, Ross W, Willey R, Cho MW, Martin MA.** 1999. Neutralizing antibody directed against the HIV-1 envelope glycoprotein can completely block HIV-1/SIV chimeric virus infections of macaque monkeys. Nat. Med. **5:**204–210. http://dx.doi.org/10.1038/5568.
50. **Burton DR, Hessell AJ, Keele BF, Klasse PJ, Ketas TA, Moldt B, Dunlop DC, Poignard P, Doyle LA, Cavacini L, Veazey RS, Moore JP.** 2011. Limited or no protection by weakly or nonneutralizing antibodies against vaginal SHIV challenge of macaques compared with a strongly neutralizing antibody. Proc. Natl. Acad. Sci. U. S. A. **108:**11181–11186. http://dx.doi.org/10.1073/pnas.1103012108.
51. **Li Y, O'Dell S, Wilson R, Wu X, Schmidt SD, Hogerkorp CM, Louder MK, Longo NS, Poulsen C, Guenaga J, Chakrabarti BK, Doria-Rose N, Roederer M, Connors M, Mascola JR, Wyatt RT.** 2012. HIV-1 neutralizing antibodies display dual recognition of the primary and coreceptor binding sites and preferential binding to fully cleaved envelope glycoproteins. J. Virol. **86:**11231–11241. http://dx.doi.org/10.1128/JVI.01543-12.
52. **Tiller T, Meffre E, Yurasov S, Tsuiji M, Nussenzweig MC, Wardemann H.** 2008. Efficient generation of monoclonal antibodies from single human B cells by single cell RT-PCR and expression vector cloning. J. Immunol. Methods **329:**112–124. http://dx.doi.org/10.1016/j.jim.2007.09.017.
53. **Larkin MA, Blackshields G, Brown NP, Chenna R, McGettigan PA, McWilliam H, Valentin F, Wallace IM, Wilm A, Lopez R, Thompson JD, Gibson TJ, Higgins DG.** 2007. Clustal W and Clustal X version 2.0. Bioinformatics **23:**2947–2948. http://dx.doi.org/10.1093/bioinformatics/btm404.
54. **Kabat EA, Wu TT, Perry HM, Gottesman KS, Foeller C.** 1991. Sequences of proteins of immunological interest, 5th ed. NIH publication no. 91-3242. National Institutes of Health, U.S. Department of Health and Human Services, Bethesda, MD.
55. **Kwon YD, Finzi A, Wu X, Dogo-Isonagie C, Lee LK, Moore LR, Schmidt SD, Stuckey J, Yang Y, Zhou T, Zhu J, Vicic DA, Debnath AK, Shapiro L, Bewley CA, Mascola JR, Sodroski JG, Kwong PD.** 2012. Unliganded HIV-1 gp120 core structures assume the CD4-bound conformation with regulation by quaternary interactions and variable loops. Proc. Natl. Acad. Sci. U. S. A. **109:**5663–5668. http://dx.doi.org/10.1073/pnas.1112391109.
56. **Otwinowski Z, Minor W.** 1997. Processing of X-ray diffraction data collected in oscillation mode. Methods Enzymol. **276:**307–326. http://dx.doi.org/10.1016/S0076-6879(97)76066-X.
57. **McCoy AJ, Grosse-Kunstleve RW, Adams PD, Winn MD, Storoni LC, Read RJ.** 2007. Phaser crystallographic software. J. Appl. Crystallogr. **40:**658–674. http://dx.doi.org/10.1107/S0021889807021206.
58. **Emsley P, Lohkamp B, Scott WG, Cowtan K.** 2010. Features and development of Coot. Acta Crystallogr. D Biol. Crystallogr. **66:**486–501. http://dx.doi.org/10.1107/S0907444910007493.
59. **Adams PD, Afonine PV, Bunkoczi G, Chen VB, Davis IW, Echols N, Headd JJ, Hung LW, Kapral GJ, Grosse-Kunstleve RW, McCoy AJ, Moriarty NW, Oeffner R, Read RJ, Richardson DC, Richardson JS, Terwilliger TC, Zwart PH.** 2010. PHENIX: a comprehensive Python-based system for macromolecular structure solution. Acta Crystallogr. D Biol. Crystallogr. **66:**213–221. http://dx.doi.org/10.1107/S0907444909052925.
60. **Krissinel E, Henrick K.** 2007. Inference of macromolecular assemblies from crystalline state. J. Mol. Biol. **372:**774–797. http://dx.doi.org/10.1016/j.jmb.2007.05.022.
61. **Chen CY, Georgiev I, Anderson AC, Donald BR.** 2009. Computational structure-based redesign of enzyme activity. Proc. Natl. Acad. Sci. U. S. A. **106:**3764–3769. http://dx.doi.org/10.1073/pnas.0900266106.
62. **Gainza P, Roberts KE, Georgiev I, Lilien RH, Keedy DA, Chen CY, Reza F, Anderson AC, Richardson DC, Richardson JS, Donald BR.** 2013. OSPREY: protein design with ensembles, flexibility, and provable algorithms. Methods Enzymol. **523:**87–107. http://dx.doi.org/10.1016/B978-0-12-394292-0.00005-9.
63. **Word JM, Lovell SC, LaBean TH, Taylor HC, Zalis ME, Presley BK, Richardson JS, Richardson DC.** 1999. Visualizing and quantifying molecular goodness-of-fit: small-probe contact dots with explicit hydrogen atoms. J. Mol. Biol. **285:**1711–1733. http://dx.doi.org/10.1006/jmbi.1998.2400.
64. **Georgiev IS, Rudicell RS, Saunders KO, Shi W, Kirys T, McKee K, O'Dell S, Chuang GY, Yang ZY, Ofek G, Connors M, Mascola JR, Nabel GJ, Kwong PD.** 2014. Antibodies VRC01 and 10E8 neutralize HIV-1 with high breadth and potency even with Ig-framework regions substantially reverted to germline. J. Immunol. **192:**1100–1106. http://dx.doi.org/10.4049/jimmunol.1302515.
65. **Chen VB, Arendall WB, III, Headd JJ, Keedy DA, Immormino RM, Kapral GJ, Murray LW, Richardson JS, Richardson DC.** 2010. MolProbity: all-atom structure validation for macromolecular crystallography. Acta Crystallogr. D Biol. Crystallogr. **66:**12–21. http://dx.doi.org/10.1107/S0907444909042073.
66. **Ahmad S, Gromiha M, Fawareh H, Sarai A.** 2004. ASAView: database and tool for solvent accessibility representation in proteins. BMC Bioinformatics **5:**51. http://dx.doi.org/10.1186/1471-2105-5-51.
67. **Dudgeon K, Rouet R, Kokmeijer I, Schofield P, Stolp J, Langley D, Stock D, Christ D.** 2012. General strategy for the generation of human antibody variable domains with increased aggregation resistance. Proc. Natl. Acad. Sci. U. S. A. **109:**10879–10884. http://dx.doi.org/10.1073/pnas.1202866109.
68. **Diskin R, Scheid JF, Marcovecchio PM, West AP, Jr, Klein F, Gao H, Gnanapragasam PN, Abadir A, Seaman MS, Nussenzweig MC, Bjorkman PJ.** 2011. Increasing the potency and breadth of an HIV antibody by using structure-based rational design. Science **334:**1289–1293. http://dx.doi.org/10.1126/science.1213782.
69. Reference deleted.
70. **Wei X, Decker JM, Liu H, Zhang Z, Arani RB, Kilby JM, Saag MS, Wu X, Shaw GM, Kappes JC.** 2002. Emergence of resistant human immunodeficiency virus type 1 in patients receiving fusion inhibitor (T-20) monotherapy. Antimicrob. Agents Chemother. **46:**1896–1905. http://dx.doi.org/10.1128/AAC.46.6.1896-1905.2002.
71. **Wu L, Zhou T, Yang ZY, Svehla K, O'Dell S, Louder MK, Xu L, Mascola JR, Burton DR, Hoxie JA, Doms RW, Kwong PD, Nabel GJ.** 2009. Enhanced exposure of the CD4-binding site to neutralizing antibodies by structural design of a membrane-anchored human immunodeficiency virus type 1 gp120 domain. J. Virol. **83:**5077–5086. http://dx.doi.org/10.1128/JVI.02600-08.
72. **Seaman MS, Janes H, Hawkins N, Grandpre LE, Devoy C, Giri A, Coffey RT, Harris L, Wood B, Daniels MG, Bhattacharya T, Lapedes A, Polonis VR, McCutchan FE, Gilbert PB, Self SG, Korber BT, Montefiori DC, Mascola JR.** 2010. Tiered categorization of a diverse panel of HIV-1 Env pseudoviruses for assessment of neutralizing antibodies. J. Virol. **84:**1439–1452. http://dx.doi.org/10.1128/JVI.02108-09.
73. **Haynes BF, Fleming J, St. Clair EW, Katinger H, Stiegler G, Kunert R,**

Robinson J, Scearce RM, Plonk K, Staats HF, Ortel TL, Liao HX, Alam SM. 2005. Cardiolipin polyspecific autoreactivity in two broadly neutralizing HIV-1 antibodies. Science **308:**1906–1908. http://dx.doi.org/10.1126/science.1111781.

74. **Ko SY, Pegu A, Rudicell RS, Yang Z-Y, Joyce MG, Chen X, Wang K, Bao S, Kraemer TD, Rath T, Zeng M, Schmidt SD, Todd JP, Penzak SR, Saunders KO, Nason MC, Haase AT, Rao SS, Blumberg RS, Mascola JR, Nabel GJ.** 2014. Enhanced neonatal Fc receptor function improves protection against primate SHIV infection. Nature. http://dx.doi.org/10.1038/nature13612.
75. **Finney DJ.** 2007. Probit analysis, 3rd ed. Cambridge University Press, Cambridge, United Kingdom.
76. **Zhu J, Ofek G, Yang Y, Zhang B, Louder MK, Lu G, McKee K, Pancera M, Skinner J, Zhang Z, Parks R, Eudailey J, Lloyd KE, Blinn J, Alam SM, Haynes BF, Simek M, Burton DR, Koff WC, NCS Program, Mullikin JC, Mascola JR, Shapiro L, Kwong PD.** 2013. Mining the antibodyome for HIV-1-neutralizing antibodies with next-generation sequencing and phylogenetic pairing of heavy/light chains. Proc. Natl. Acad. Sci. U. S. A. **110:**6470–6475. http://dx.doi.org/10.1073/pnas.1219320110.
77. **Kwong PD, Wyatt R, Robinson J, Sweet RW, Sodroski J, Hendrickson WA.** 1998. Structure of an HIV gp120 envelope glycoprotein in complex with the CD4 receptor and a neutralizing human antibody. Nature **393:**648–659. http://dx.doi.org/10.1038/31405.
78. **Zalevsky J, Chamberlain AK, Horton HM, Karki S, Leung IW, Sproule TJ, Lazar GA, Roopenian DC, Desjarlais JR.** 2010. Enhanced antibody half-life improves in vivo activity. Nat. Biotechnol. **28:**157–159. http://dx.doi.org/10.1038/nbt.1601.
79. **Kontermann RE.** 2009. Strategies to extend plasma half-lives of recombinant antibodies. BioDrugs **23:**93–109. http://dx.doi.org/10.2165/00063030-200923020-00003.
80. **Tang L, Persky AM, Hochhaus G, Meibohm B.** 2004. Pharmacokinetic aspects of biotechnology products. J. Pharm. Sci. **93:**2184–2204. http://dx.doi.org/10.1002/jps.20125.
81. **Horwitz JA, Halper-Stromberg A, Mouquet H, Gitlin AD, Tretiakova A, Eisenreich TR, Malbec M, Gravemann S, Billerbeck E, Dorner M, Buning H, Schwartz O, Knops E, Kaiser R, Seaman MS, Wilson JM, Rice CM, Ploss A, Bjorkman PJ, Klein F, Nussenzweig MC.** 2013. HIV-1 suppression and durable control by combining single broadly neutralizing antibodies and antiretroviral drugs in humanized mice. Proc. Natl. Acad. Sci. U. S. A. **110:**16538–16543. http://dx.doi.org/10.1073/pnas.1315295110.
82. **Klein F, Mouquet H, Dosenovic P, Scheid JF, Scharf L, Nussenzweig MC.** 2013. Antibodies in HIV-1 vaccine development and therapy. Science **341:**1199–1204. http://dx.doi.org/10.1126/science.1241144.
83. **Voronin Y, Mofenson LM, Cunningham CK, Fowler MG, Kaleebu P, McFarland EJ, Safrit JT, Graham BS, Snow W.** 2014. HIV monoclonal antibodies: a new opportunity to further reduce mother-to-child HIV transmission. PLoS Med. **11:**e1001616. http://dx.doi.org/10.1371/journal.pmed.1001616.
84. **Mehandru S, Vcelar B, Wrin T, Stiegler G, Joos B, Mohri H, Boden D, Galovich J, Tenner-Racz K, Racz P, Carrington M, Petropoulos C, Katinger H, Markowitz M.** 2007. Adjunctive passive immunotherapy in human immunodeficiency virus type 1-infected individuals treated with antiviral therapy during acute and early infection. J. Virol. **81:**11016–11031. http://dx.doi.org/10.1128/JVI.01340-07.
85. **Trkola A, Kuster H, Rusert P, Joos B, Fischer M, Leemann C, Manrique A, Huber M, Rehr M, Oxenius A, Weber R, Stiegler G, Vcelar B, Katinger H, Aceto L, Gunthard HF.** 2005. Delay of HIV-1 rebound after cessation of antiretroviral therapy through passive transfer of human neutralizing antibodies. Nat. Med. **11:**615–622. http://dx.doi.org/10.1038/nm1244.
86. **Joos B, Trkola A, Kuster H, Aceto L, Fischer M, Stiegler G, Armbruster C, Vcelar B, Katinger H, Gunthard HF.** 2006. Long-term multiple-dose pharmacokinetics of human monoclonal antibodies (MAbs) against human immunodeficiency virus type 1 envelope gp120 (MAb 2G12) and gp41 (MAbs 4E10 and 2F5). Antimicrob. Agents Chemother. **50:**1773–1779. http://dx.doi.org/10.1128/AAC.50.5.1773-1779.2006.
87. **Wu H, Pfarr DS, Johnson S, Brewah YA, Woods RM, Patel NK, White WI, Young JF, Kiener PA.** 2007. Development of motavizumab, an ultra-potent antibody for the prevention of respiratory syncytial virus infection in the upper and lower respiratory tract. J. Mol. Biol. **368:**652–665. http://dx.doi.org/10.1016/j.jmb.2007.02.024.
88. **Hessell AJ, Hangartner L, Hunter M, Havenith CE, Beurskens FJ, Bakker JM, Lanigan CM, Landucci G, Forthal DN, Parren PW, Marx PA, Burton DR.** 2007. Fc receptor but not complement binding is important in antibody protection against HIV. Nature **449:**101–104. http://dx.doi.org/10.1038/nature06106.
89. **Moldt B, Schultz N, Dunlop DC, Alpert MD, Harvey JD, Evans DT, Poignard P, Hessell AJ, Burton DR.** 2011. A panel of IgG1 b12 variants with selectively diminished or enhanced affinity for Fcgamma receptors to define the role of effector functions in protection against HIV. J. Virol. **85:**10572–10581. http://dx.doi.org/10.1128/JVI.05541-11.